MISCELLANEOUS PAPER S-72-1

X-RAY MEASUREMENT OF SOIL DENSITIES IN MODELS

by

E. L. Krinitzsky

D D C

FEB 16 1972

January 1972

54

DOCUMENT CONTROL DATA - R & D

(Security classification of title, body of abstract and indexing annotation must be entered when the overall report is classified)

1. ORIGINATING ACTIVITY *(Corporate author)*	2a. REPORT SECURITY CLASSIFICATION
U. S. Army Engineer Waterways Experiment Station Vicksburg, Mississippi	Unclassified
	2b. GROUP

3. REPORT TITLE

X-RAY MEASUREMENT OF SOIL DENSITIES IN MODELS

4. DESCRIPTIVE NOTES *(Type of report and inclusive dates)*
Final report

5. AUTHOR(S) *(First name, middle initial, last name)*

Ellis L. Krinitzsky

6. REPORT DATE	7a. TOTAL NO. OF PAGES	7b. NO. OF REFS
January 1972	52	3

8a. CONTRACT OR GRANT NO.	9a. ORIGINATOR'S REPORT NUMBER(S)
b. PROJECT NO. 6.11.01.A-4A061101A91D, Item AZ	Miscellaneous Paper S-72-1
c.	9b. OTHER REPORT NO(S) *(Any other numbers that may be assigned this report)*
d.	

10. DISTRIBUTION STATEMENT

Approved for public release; distribution unlimited

11. SUPPLEMENTARY NOTES	12. SPONSORING MILITARY ACTIVITY
	Assistant Secretary of the Army (R&D) Department of the Army Washington, D. C.

13. ABSTRACT

Film density measurements of X-radiographs can be interpreted into soil density measurements under suitable controlled conditions and with proper calibration curves. The method is nondestructive, and determinations can be made for a model during various stages of testing. The method needs to be supplemented to observe deformation and shear planes.

DD FORM 1473 REPLACES DD FORM 1473, 1 JAN 64, WHICH IS OBSOLETE FOR ARMY USE.

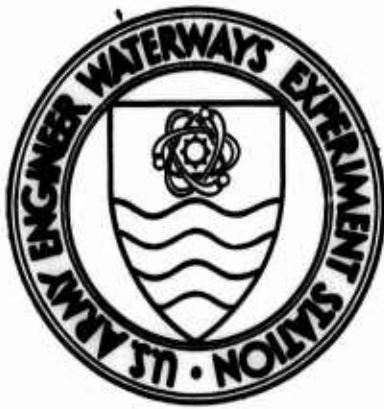Destroy this report when no longer needed. Do not return
it to the originator.

The findings in this report are not to be construed as an official
Department of the Army position unless so designated
by other authorized documents.

14. KEY WORDS	LINK A		LINK B		LINK C	
	ROLE	WT	ROLE	WT	ROLE	WT
Models						
Soil density						
X-radiography						

X-RAY MEASUREMENT OF SOIL DENSITIES IN MODELS

by

E. L. Krinitzsky

January 1972

FOREWORD

CONTENTS

CONVERSION FACTORS, BRITISH TO METRIC UNITS OF MEASUREMENT

British units of measurement used in this report can be converted to metric units as follows:

Multiply	By	To Obtain
inches	2.54	centimeters
square inches	6.4516	square centimeters
Fahrenheit degrees	5/9	Celsius or Kelvin degrees*

---

* To obtain Celsius (C) temperature readings from Fahrenheit (F) readings, use the following formula: $C = (5/9)(F - 32)$. To obtain Kelvin (K) readings, use: $K = (5/9)(F - 32) + 273.15$.

SUMMARY

Film density measurements of X-radiographs can be interpreted into
soil density measurements under suitable controlled conditions and with
proper calibration curves. The method is nondestructive, and determina-
tions can be made for a model during various stages of testing. The
method needs to be supplemented to observe deformation and shear planes.

BLANK PAGE

X-RAY MEASUREMENT OF SOIL DENSITIES IN MODELS

PART I: INTRODUCTION

Radiography

1. Radiography is the use of penetrating radiation to produce shadow images of the internal structure of materials. As a technique it has been in use since Roentgen made his discovery of X-rays in 1895. However, applications in soils engineering have been comparatively slow in developing.

2. Movements of lead pellets in sand during a plate bearing test were first monitored in 1929. Gradually radiography was applied to other tests including those on footings, compaction of soils, strain in sand, effects of pile penetrations, and displacements under moving wheel loads. Recently, such work has broadened greatly, but it has been concentrated on observing physical displacements. Until now, very little has been done in utilizing the quantitative aspects of radiographic imagery for analyzing density changes in soils. The present discussion relates specifically to this problem.

3. Film density in a radiographic image of a soil model is a measure of soil density in the material that is radiographed. The principle involved is that radiation absorption is a function of the chemical composition and the mass of the material that is radiated.

4. The radiographic image is also influenced by other factors. These are:

        a. Variation in thickness of the specimen.

        b. Nonuniformity in mineralogical composition.

        c. Irregularities in the shape of X-ray beam.

        d. Irregularities in the energy input to the X-ray tube.

        e. Variations in the chemical bath used for film developing.

        f. Scatter and undercutting that are dependent on the shape and materials of the model.

These factors need to be evaluated properly, and corrections must be made for the errors they contribute.

Purpose of This Study

5. The present evaluations were made and experiments were run in order to show how soil densities can be interpreted successfully by radiographic means and how possible causes of errors can be recognized and corrected.

Advantages of Radiographic Measurements

6. The advantages of making radiographic measurements of densities of soil models are several:

<u>a</u>. Radiographic measurements are nondestructive. Hence, determinations can be made at intervals during the progression of a test, without interfering with the model.

<u>b</u>. Determinations can be made for small areas, as small as a few microns across. Also, scanning can be done in ways that provide accurate contours of complex patterns of density changes that are unobtainable by any other method.

<u>c</u>. Density changes can be related to other features, such as patterns of plastic deformation, the initiation and growth of shear planes, and progressions in the mechanism of residual shear.

7. These capabilities, in turn, are especially useful for the following applications:

<u>a</u>. Basic research in the fundamentals of strength testing.

<u>b</u>. Model studies of strain and stress relations.

<u>c</u>. Effects of geological characteristics, or natural features in undisturbed samples, on strength testing.

<u>d</u>. Effects of boundary conditions on soil deformation.

Equipment and Materials Used

8. Radiation for the experiments described herein was provided by a Philips Industrial X-Ray Unit using a 100-kv beryllium window tube with a copper target. Registration was on Kodak type M industrial X-ray film presealed in Ready-Pack envelopes. A Joyce-Loebl Isodensitracer was used to enhance and measure the radiographic images. A MacBeth Quantalog Photodensitometer was used for additional measurements.

2

PART II: CALCULATION OF RADIATION ABSORPTION

Exponential Decay Equation

9. Absorption of X-rays passing through a material can be calculated by the exponential decay equation

$$I = I_o e^{-\mu x}$$

where

    I = intensity of transmitted radiation

    I_o = intensity of incident radiation

    μ = absorption coefficient

    x = path length through the material

Absorption Coefficient

10. The absorption coefficient for a pure material such as a metal cast homogeneously can be obtained very easily from tables. For soils, in which the mineralogy may be complex and the chemical constituents of individual minerals may also be complex, the absorption coefficient must be expressed as a sum of the coefficients for each constituent element in the soil and in terms of the densities of the minerals and the density of the aggregate mass. Thus, the exponential decay equation is written

$$I = I_o e^{-(\mu/\rho)\rho_T x}$$

where

    μ/ρ = the mass absorption coefficient for the minerals composing a soil

    ρ_T = the density of the soil mass

11. The coefficients for mass absorption of radiation vary for different levels of radiation energy. Fig. 1 shows the variations in coefficients for a group of the common elements according to changes in
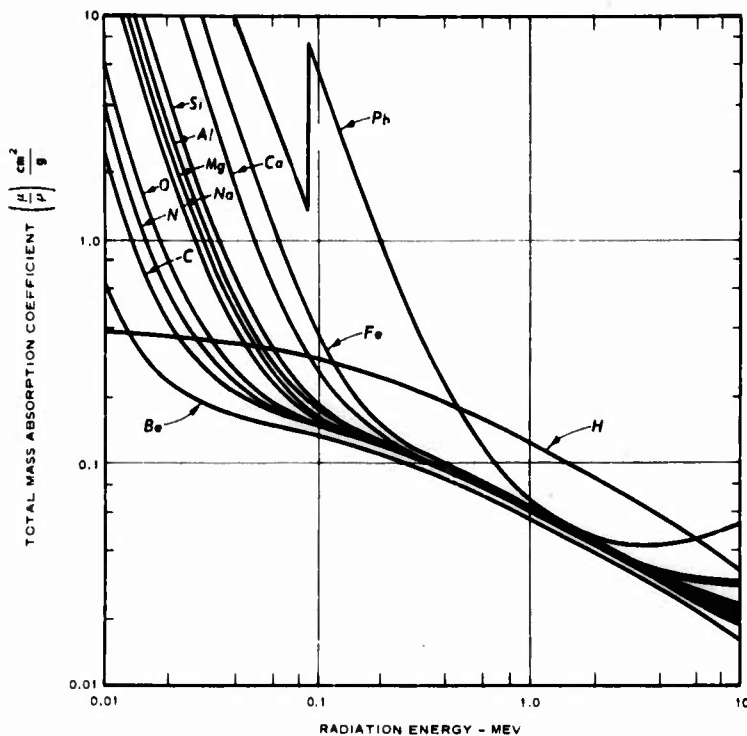
3

Fig. 1. Mass absorption coefficients versus radiation energy for selected elements. (After Bloedow, 1962)

radiation energy. These curves were prepared by Bloedow[*] from the comprehensive tables published by McMaster.[**] McMaster's tables itemize the individual effects of scattering photoelectric changes, and pair formation that X-rays are subject to when they pass through materials. His tables also show the total mass absorption and the linear absorption for a range of energy levels common to radiographic work. His tables cover all of the common elements.

12. Calculation of the mass absorption coefficient μ/ρ for a complex mineral or a group of minerals using tables that show only the values for individual elements is done by summation:

$$\left(\frac{\mu}{\rho}\right)_{compound} = R_1\left(\frac{\mu}{\rho}\right)_1 + R_2\left(\frac{\mu}{\rho}\right)_2 + \ldots + R_n\left(\frac{\mu}{\rho}\right)_n$$

---

[*] F. H. Bloedow, "Radiographic Instrumentation Study," AFSWC-TDR-62-44, 1962, Kirtland Air Force Base, N. Mex.

[**] R. C. McMaster, ed., Attenuation Coefficient Tables, Nondestructive Testing Handbook, Vol. 1, Part 27, The Ronald Press, New York, 1959, pp 1-41.

where

$\left(\dfrac{\mu}{\rho}\right)_1$ = mass absorption coefficient of element 1 for a given energy of radiation

R_1 = ratio of the atomic weight of element 1 in the compound to the total atomic weight of the compound

An example for the calculation of the mass absorption coefficient at a given energy level for kaolinite $(2H_2O.Al_2O_3.SiO_2)$ is given below from Bloedow.

ELEMENT	NUMBER OF ATOMS	ATOMIC WEIGHT	ATOMIC WEIGHT IN COMPOUND	R	MASS ABSORPTION COEFFICIENT OF ELEMENT AT 300 KEV	$R\left(\dfrac{\mu}{\rho}\right)$
HYDROGEN	4	1	4	0.0202	0.212	0.0043
OXYGEN	7	16	112	0.5657	0.107	0.0605
ALUMINUM	2	27	54	0.2727	0.104	0.0284
SILICON	1	28	28	0.1414	0.108	0.0153
ATOMIC WEIGHT OF COMPOUND = 198				1.0000	$\left(\dfrac{\mu}{\rho}\right)$ COMPOUND = 0.1085	

13. With the determination of μ/ρ , the exponential decay equation can be solved to determine the change in intensity of the X-ray beam when it passes through a specimen of kaolinite of a given density.

14. For multiple layers, the equation can be stated as

$$I = I_o e^{-\left(\frac{\mu}{\rho}\rho_T x\right)_1 - \left(\frac{\mu}{\rho}\rho_T x\right)_2 - \cdots -\left(\frac{\mu}{\rho}\rho_T x\right)_n}$$

Calculation Difficulties

15. From this it can be seen that measurements of incident radiation from degree of film darkening (photodensity) would then be relatable directly to soil density. Such calculations can be made with some reasonable assurance of reliability when the material is a metal or a known mixture of metals, but for soils there are complexities that cannot be easily resolved.

16. Often the chemical formula for a mineral, particularly when it is a clay, is a simplification. Water within the crystal lattice is a

5

variable quantity. And in natural soils, there very seldom is only one clay mineral present. Rather there are several, plus minor amounts of a great variety of other constituents. Calculations then would have to be made on the basis of broad assumptions, and those assumptions might not allow the degree of accuracy that is desired in the subsequent testing.

17. There is an unevaluated effect of high pore space in soils. Fraser and James* found a linearity in exposure versus thickness measurements in dense shales but found no such linearity in less dense marine muds. Fraser and James suggest that pore spaces in soils cause changes in the linear absorption coefficient as the beams pass from mineral particles to interstitial space. Porosity may present many surfaces that aid the dissipation of energy through scatter.

18. Calculations also leave unresolved other problems that derive from effects of the shape and materials of the models, vagaries in energy levels, changes in the chemical baths, etc. These are discussed more fully in the following sections.

19. At this point it is sufficient to say that calculations alone are not a satisfactory means for evaluating soil densities.

---

* G. S. Fraser and A. T. James, "Radiographic Exposure Guides for Mud, Sandstone, Limestone, and Shale," Illinois State Geological Survey Circular 443, 1969, Urbana, Illinois.

20.   In order to use a radiographic film image as a measure of soil density, several sources of error must be kept in mind.

Position of X-Ray Beam

21.   It is known that radiation intensities may not be equitably distributed over the area exposed to radiation.   Fig. 2 shows what is
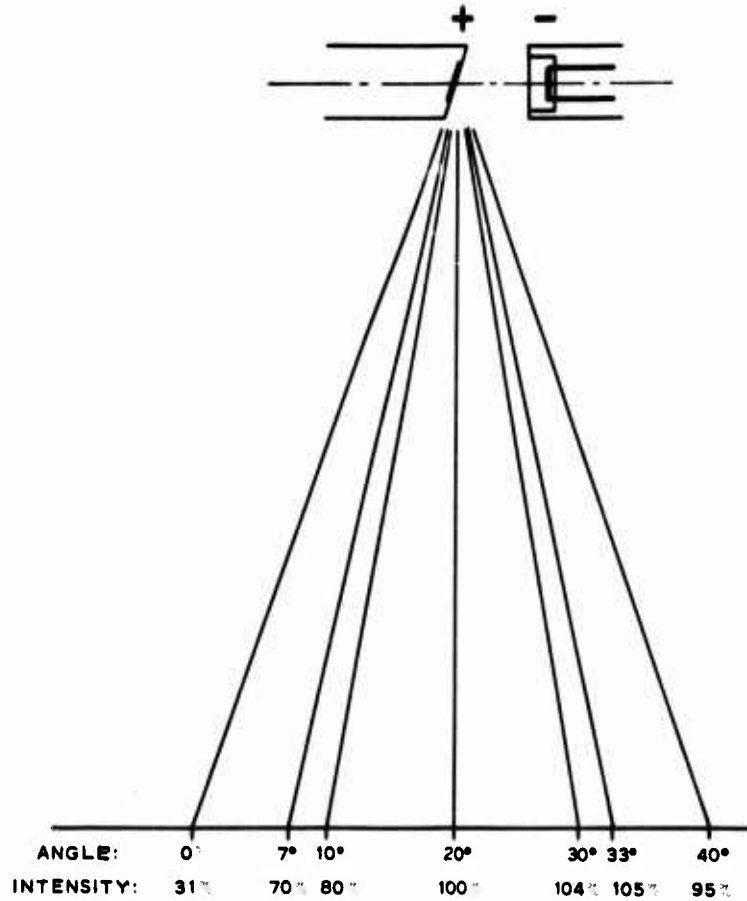
Fig. 2. Variations of radiation intensity in terms of angle of emergence. (After McMaster, 1959)

ANGLE:	0	7° 10°	20°	30° 33°	40°
INTENSITY:	31%	70% 80%	100%	104% 105%	95%

called a "heel" effect, or a heightening in the intensity of radiation that occurs in one portion of the area, plus a variation in the spread of the intensities.   These patterns of radiation intensity occur with a reasonable sameness from exposure to exposure.   Thus, correction for their effect can be made empirically.   It is essential that all exposure for a series of tests be made in identical positions, and a control radiograph

must be made of the model in an untested condition.

22. If a tested area is small, it can be found by means of the control radiograph that the uniformity of radiation is sufficient for the experiment.

23. For larger areas, photodensity values from the control radiograph can be removed from each of the test radiographs. The values then remaining would be residual values. They would measure degrees of disturbance. They could be interpreted by means of a calibration chart to give soil density values.

24. For some model configurations, e.g. small rings or disks, photodensity values can be averaged and a base line made. Changes in values can then be measured as movements of these base lines.
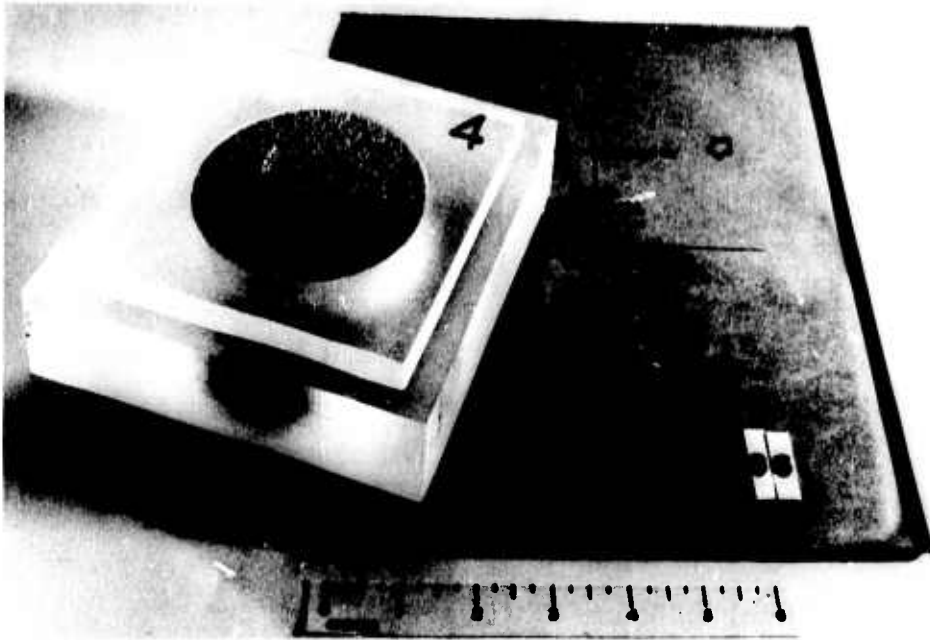
25. In any event, radiation patterns are not inhibitions to testing, provided that their effects are controlled and accounted for.
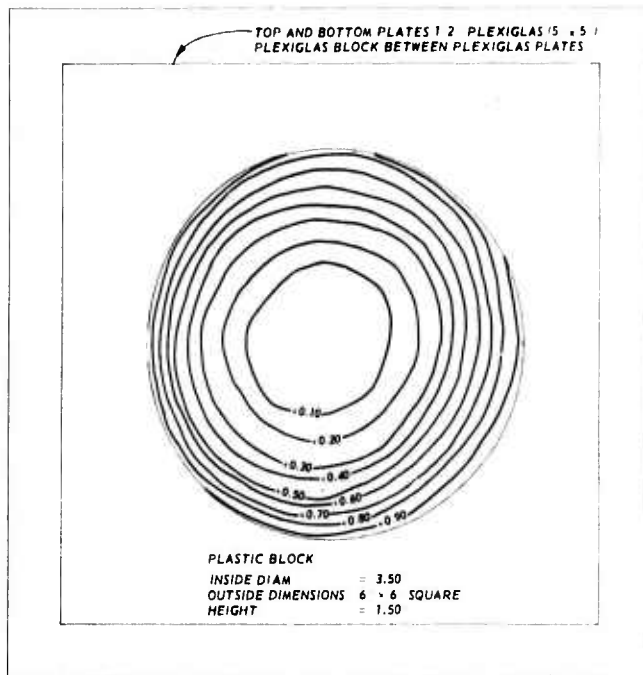
Scatter and Undercutting in Models

26. A prime source of error in soil models is from radiation scatter and undercutting caused by the materials and the shapes of the models themselves. Following are experiments that illustrate this point. In all of the tests, the cylindrical interior volume of sand was the same. However, the containers around the sand were varied.

27. First, the sand was contained within a block of plexiglas and was covered above and below with plates of plexiglas, see fig. 3a. The dimensions* and exposure conditions are shown in fig. 3b. Also shown is the pattern of radiation scatter. The values are in terms of film density units. They are residuals left after the removal of an interpreted base line. The base line was taken from an average of the interior values in the sample where changes in values were least pronounced and where outside effects were considered to be at a minimum.

---

* The dimensions are shown in this and certain subsequent illustrations in British units of measurement. Also, some dimensions in the ensuing text are in British units. These units can be converted to metric units by use of the table given on page ix.

8

a.   Sand model

TOP AND BOTTOM PLATES 1 2 PLEXIGLAS (5 . 5)
PLEXIGLAS BLOCK BETWEEN PLEXIGLAS PLATES

PLASTIC BLOCK
INSIDE DIAM   = 3.50
OUTSIDE DIMENSIONS   6 . 6 SQUARE
HEIGHT   = 1.50

SAND DENSITY 1.74, FILM DENSITY 1.01
CONTOURS INDICATE DEVIATION FROM BASE FILM DENSITY
9 MA, 69 KV, 60 SEC, 33-IN. F.D., KODAK TYPE M FILM

PATTERN OF RADIATION SCATTER
SAMPLE 87
OTTAWA SAND (20 TO 28 MESH)

b.   Excessive undercutting by radiation has
resulted from the plexiglas container

Fig. 3.   Sand model formed from a block of plexiglas and covered
with plexiglas plates, and pattern of radiation scatter

28. The residual values vary from zero in the central portion of the sand to +0.90 along the periphery. This range is much too great to allow in soils tests, as induced changes would be much less than this spread of values. Corrections, with variations of this magnitude, would have a range of possible error that is greater than postulated changes in the model.

29. The reason for the great variation is that the plastic container permits excessive undercutting by radiation. It follows that models constructed of this material will behave unsatisfactorily.

30. In order to reduce this problem, the plexiglas block was replaced by an aluminum ring. Aluminum absorbs radiation more effectively than plexiglas; hence, it acts to restrain undercutting along the periphery of the sand. A view of the model is shown in fig. 4a. The effects of undercutting on the radiographic image are shown in figs. 4b and 4c. The undercutting shows up visually in the print from the radiograph in fig. 4b. (Remember that the lightening along the edges of the sand comes from a radiograph in which there is darkening.) The values for deviation from a base line (fig. 4c) are as great as +0.35. This is a significant reduction from the +0.90 produced by the plexiglas block. A test to confirm the unwanted effect of a plexiglas sidewall was made by substituting a plexiglas ring for the aluminum ring (see fig. 4d). Again variations are up to +0.70 and +0.80 of a density unit.

31. Referring again to fig. 4c, we may note a complication of a different sort in the pattern of film density values. The pattern is not circular. It is very crudely squarelike. This squarelike pattern was not observed in figs. 3b or 4d because of the strong undercutting that came from all directions. In fig. 4c, it is possible to observe a smaller effect that is at work. Fig. 4e shows a further explanation of this effect. The model has been turned 45 deg and radiated. Note that the blocklike pattern in the residual values also has been turned 45 deg. Thus, this effect does not result from any pattern originating in the X-ray tube. It originates in the model. It is an undercutting effect that is contributed by the square shapes of the upper and lower plexiglas plates. Fig. 4f further explores this condition with a rotation of these

10

TOP AND BOTTOM PLATES 1/2" PLEXIGLAS (5" × 5")
ALUMINUM RING BETWEEN PLEXIGLAS PLATES

ALUMINUM RING

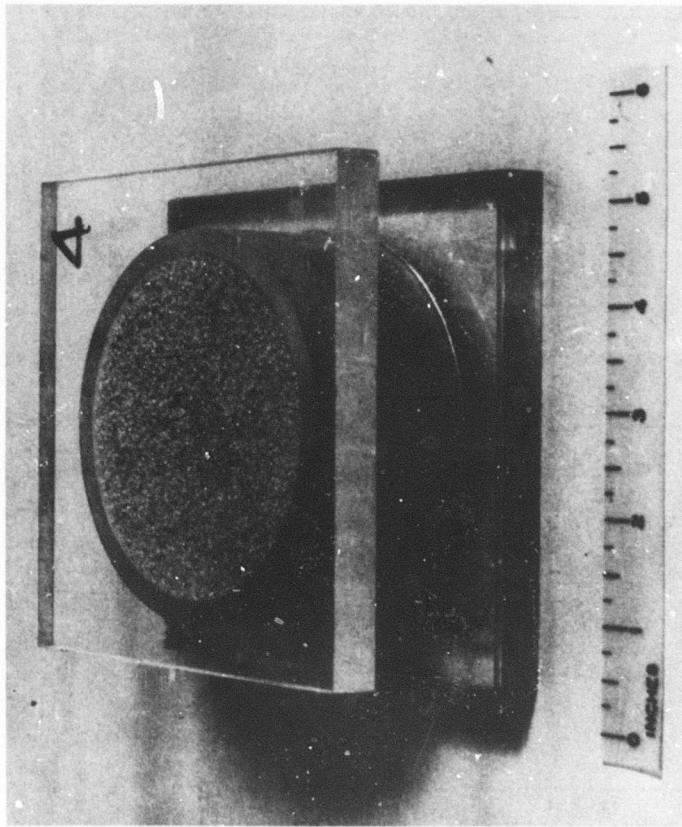INSIDE DIAM = 3.50"
OUTSIDE DIAM = 4.00"
HEIGHT   = 1.50"

SAND DENSITY: 1.84; FILM DENSITY: 0.51

9 MA, 69 KV, 60 SEC, 33-IN. F.D., KODAK TYPE M FILM

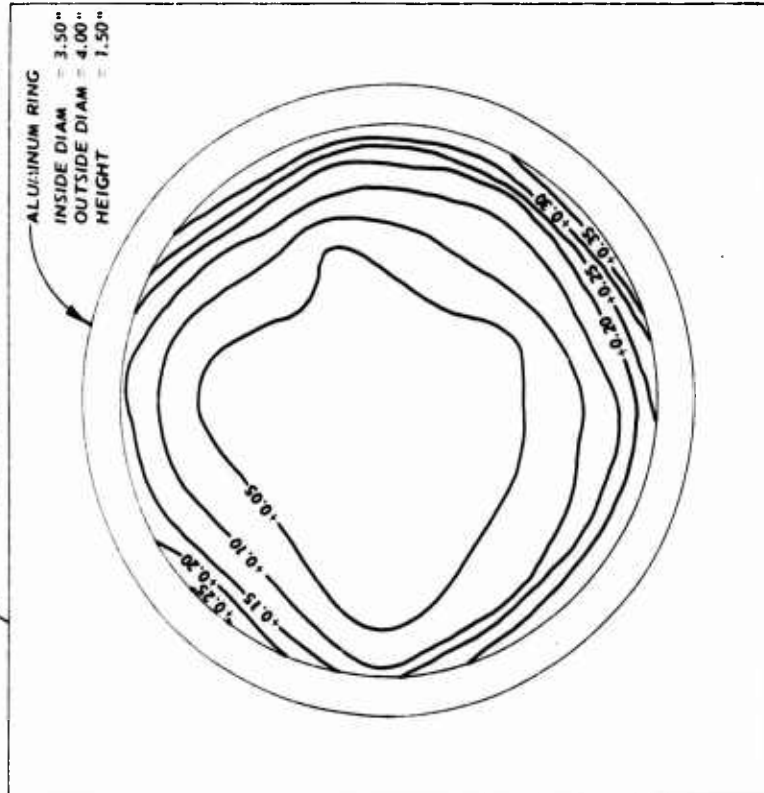PATTERN OF RADIATION SCATTER

SAMPLE 13

OTTAWA SAND (20 TO 28 MESH)

b. Radiation scatter and undercutting.
    (Print made from radiographic image)

a. Sand model

Fig. 4. Sand model formed from an aluminum ring between square plexiglas plates, pattern of radia-
tion scatter, and film density variations before and after various model modifications (sheet 1 of 3)
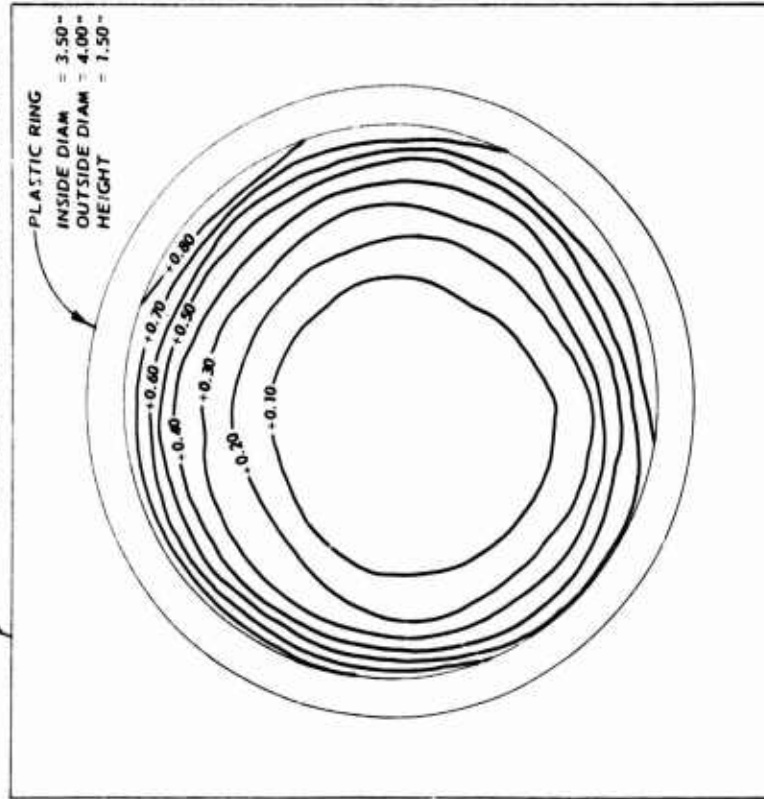
PATTERN OF RADIATION SCATTER

SAND DENSITY: 1.76, FILM DENSITY: 0.90

CONTOURS INDICATE DEVIATION FROM BASE FILM DENSITY:
9 MA, 69 KV, 60 SEC, 33-IN. F.D., KODAK TYPE M FILM

PLASTIC RING

INSIDE DIAM = 3.50"
OUTSIDE DIAM = 4.00"
HEIGHT = 1.50"

TOP AND BOTTOM PLATES 1/2 PLEXIGLAS (5 × 5)
PLEXIGLAS RING BETWEEN PLEXIGLAS PLATES

SAMPLE 88

OTTAWA SAND (20 TO 28 MESH)

+0.80
+0.70
+0.60
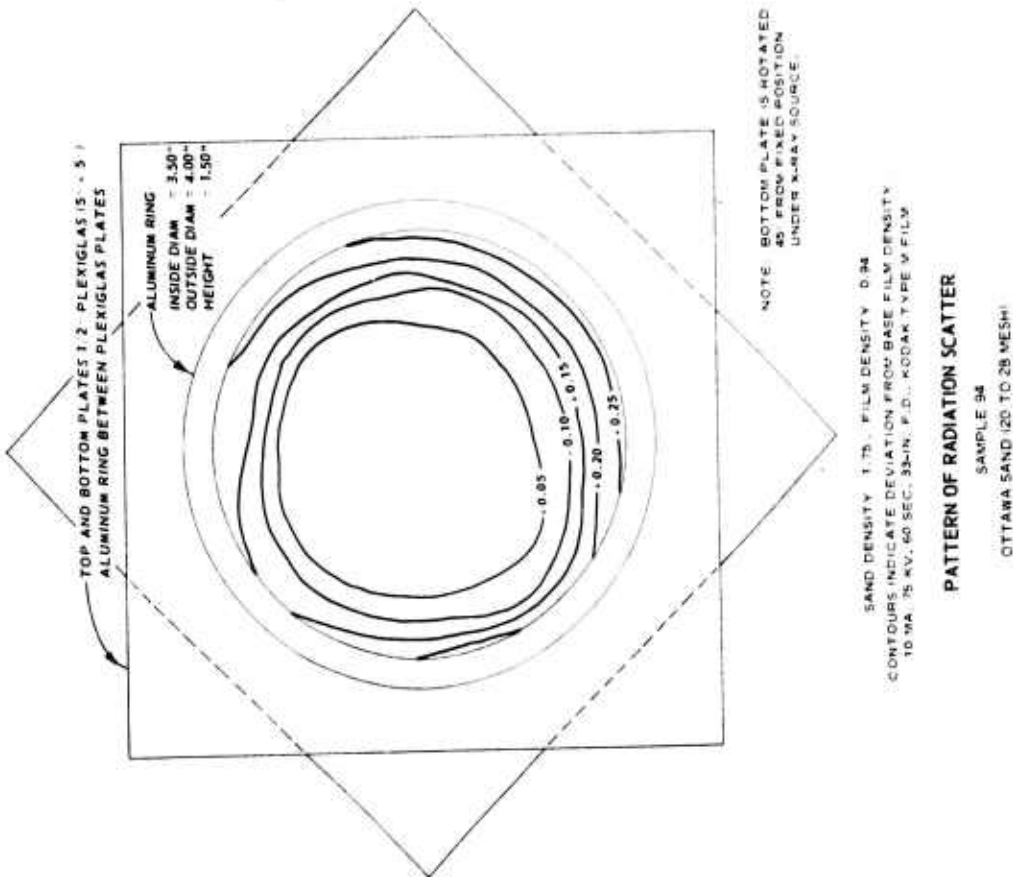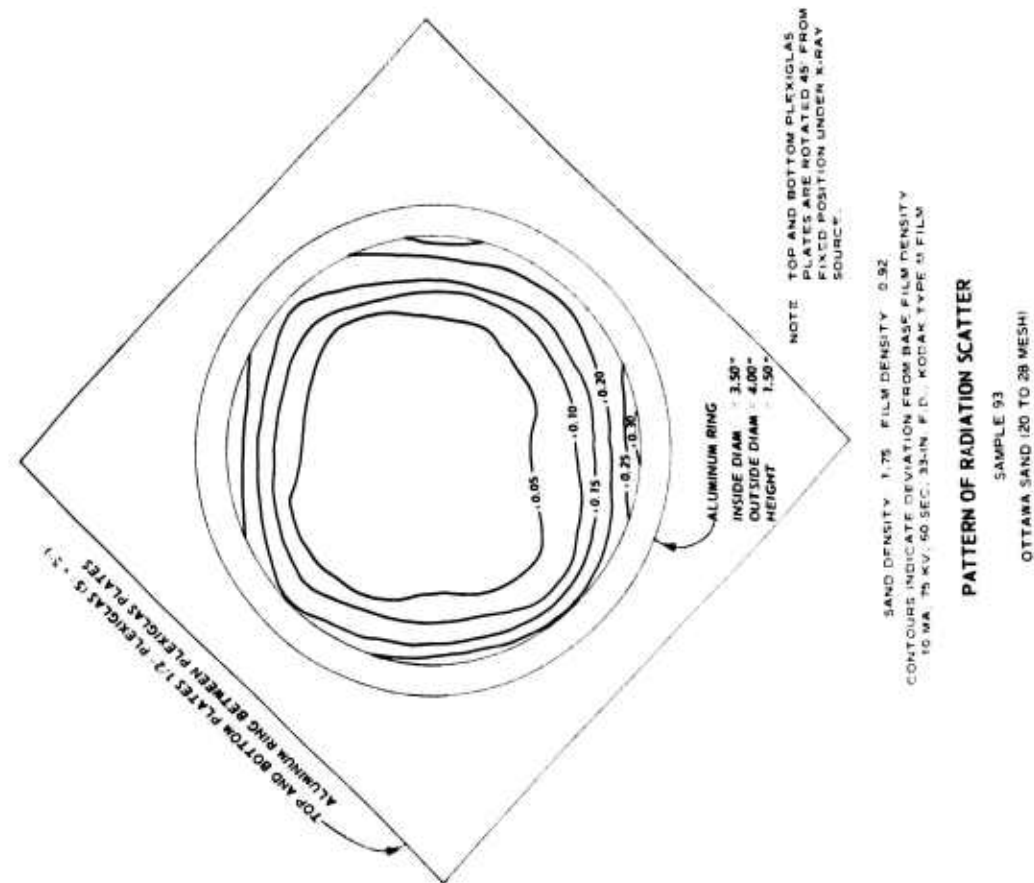+0.50
+0.40
+0.30
+0.20
+0.10

PATTERN OF RADIATION SCATTER

SAND DENSITY: 1.84; FILM DENSITY: 0.51

CONTOURS INDICATE DEVIATION FROM BASE FILM DENSITY:
9 MA, 69 KV, 60 SEC, 33-IN. F.D., KODAK TYPE M FILM

ALUMINUM RING

INSIDE DIAM = 3.50"
OUTSIDE DIAM = 4.00"
HEIGHT = 1.50"

TOP AND BOTTOM PLATES 1/2 PLEXIGLAS (5 × 5)
ALUMINUM RING BETWEEN PLEXIGLAS PLATES

SAMPLE 13

OTTAWA SAND (20 TO 28 MESH)

-0.05
-0.10
-0.15
-0.20
-0.25
-0.30

c. Residual values of film density variation.
Note the noncircular pattern of the contours

d. Excessive film density variations produced
by plastic ring

Fig. 4 (sheet 2 of 3)

12

TOP AND BOTTOM PLATES 1-2 PLEXIGLAS (5" × 5")
ALUMINUM RING BETWEEN PLEXIGLAS PLATES

ALUMINUM RING
INSIDE DIAM = 3.50"
OUTSIDE DIAM = 4.00"
HEIGHT = 1.50"

NOTE: BOTTOM PLATE IS ROTATED 45° FROM FIXED POSITION UNDER X-RAY SOURCE.

SAND DENSITY 1.75. FILM DENSITY 0.94
CONTOURS INDICATE DEVIATION FROM BASE FILM DENSITY
10 MA. 75 KV. 60 SEC. 33-IN. F.D. KODAK TYPE M FILM

PATTERN OF RADIATION SCATTER

SAMPLE 94

OTTAWA SAND (20 TO 28 MESH)

f. Film density variations produced with covering plates rotated 45 deg to each other

TOP AND BOTTOM PLEXIGLAS PLATES ARE ROTATED 45° FROM FIXED POSITION UNDER X-RAY SOURCE.

ALUMINUM RING
INSIDE DIAM = 3.50"
OUTSIDE DIAM = 4.00"
HEIGHT = 1.50"

SAND DENSITY 1.75. FILM DENSITY 0.92
CONTOURS INDICATE DEVIATION FROM BASE FILM DENSITY
10 MA. 75 KV. 60 SEC. 33-IN. F.D. KODAK TYPE M FILM

PATTERN OF RADIATION SCATTER

SAMPLE 93

OTTAWA SAND (20 TO 28 MESH)

TOP AND BOTTOM PLATES 1-2 PLEXIGLAS (5" × 5")
ALUMINUM RING BETWEEN PLEXIGLAS PLATES

e. Square contours of film density variations produced by square covering plates

Fig. 4 (sheet 3 of 3)

13

plates of 45 deg to each other. It is noted that the square effect in the residual values has been reduced, though it has not been eliminated as there now are octagonal corners that contribute their effects, especially from corners of the top plate.

32. It was noted in fig. 4d that a plexiglas ring permitted undercutting of the radiographic image to +0.70 and +0.80 of a photodensity unit. Fig. 5a shows the same model; however, the plastic ring has been sheathed with lead. The pattern of residual values that was produced by this ring is shown in fig. 5b. The lead sheath reduced undercutting by two-thirds. The central area in which undercutting effects did not occur was significantly increased.

33. Figs. 6a and 6b show the application of lead sheathing to the aluminum ring. The results in fig. 6b provide a uniformity of film density that is within a few hundredths of a film density unit. The lead sheath around the ring not only reduced undercutting to a negligible quantity but here, and in fig. 5b, it also reduced the effects on the sample of the square covering plates.

34. The plastic covering plates were made circular and were fitted to the aluminum ring and the lead sheath for the experiments illustrated in figs. 7a-7c. The resulting patterns are on the order of a tenth of a film density unit in fig. 7b for a sand density of 1.77 and less than a tenth of a unit in fig. 7c for a sand density of 1.82. The comparison suggests that a denser material may develop less registration spread than the same material in a less dense condition. The experiments suggest also that the lateral barrier to radiation undercutting provided by the lead and aluminum rings is the important factor in controlling irregularities. The shape of the cover plates does not matter if the lateral containment is of a proper design.

35. A final experiment was made to determine if a lead cover plate with an overhang that covered part of the sample was of any further aid in controlling irregularities in registration of radiation. The lead cover was placed on the aluminum ring with its lead sheath (figs. 8a and 8b). The experiment, fig. 8b, showed that the results were kept within a manageable degree of accuracy. Residual values were somewhat

14
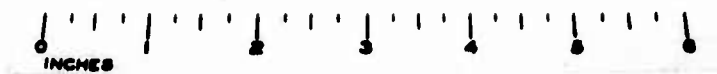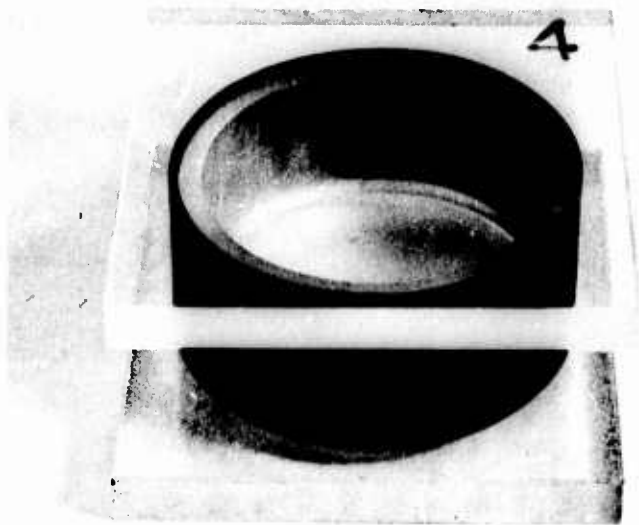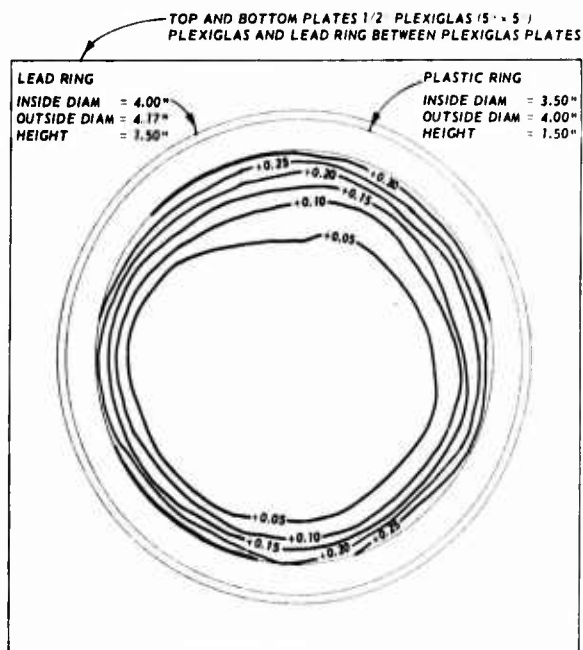
a. Model

SAND DENSITY 1.69, FILM DENSITY 1.42
CONTOURS INDICATE DEVIATION FROM BASE FILM DENSITY
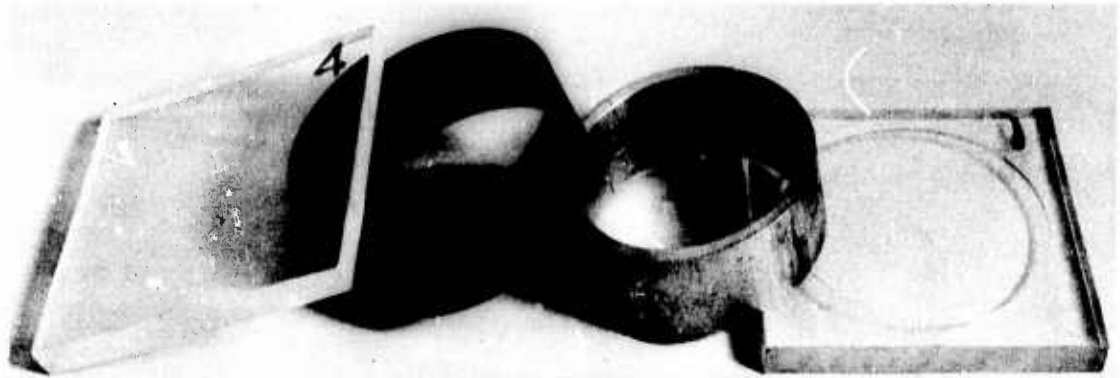5 MA, 90 KV, 60 SEC, 33-IN. F.D., KODAK TYPE M FILM
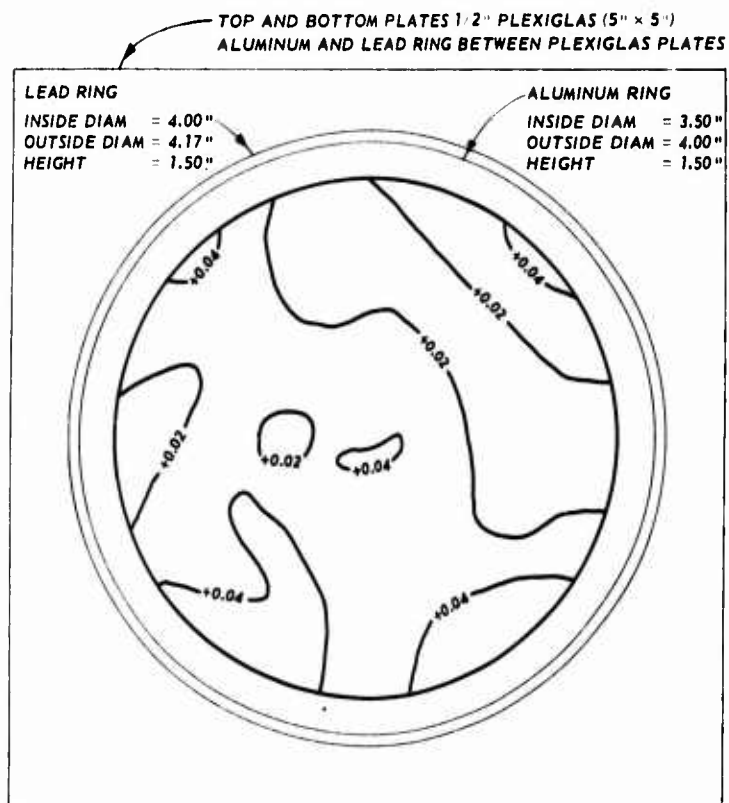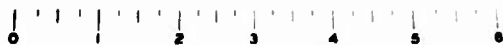
PATTERN OF RADIATION SCATTER

SAMPLE 71

OTTAWA SAND (20 TO 28 MESH)

b. Film density variations

Fig. 5. Model with plexiglas ring shielded with an
outer lead sheath, and film density variations

a. Model

TOP AND BOTTOM PLATES 1/2" PLEXIGLAS (5" × 5")
ALUMINUM AND LEAD RING BETWEEN PLEXIGLAS PLATES

LEAD RING
INSIDE DIAM   = 4.00"
OUTSIDE DIAM = 4.17"
HEIGHT   = 1.50"

ALUMINUM RING
INSIDE DIAM   = 3.50"
OUTSIDE DIAM = 4.00"
HEIGHT   = 1.50"

SAND DENSITY: 1.70, FILM DENSITY: 1.27
CONTOURS INDICATE DEVIATION FROM BASE FILM DENSITY:
5 MA, 90 KV, 60 SEC, 33-IN. F.D., KODAK TYPE M FILM

PATTERN OF RADIATION SCATTER

SAMPLE 68

OTTAWA SAND (20 TO 28 MESH)

b. Film density variations. (Note the low
order of these variations)

Fig. 6. Model of aluminum ring with lead sheath,
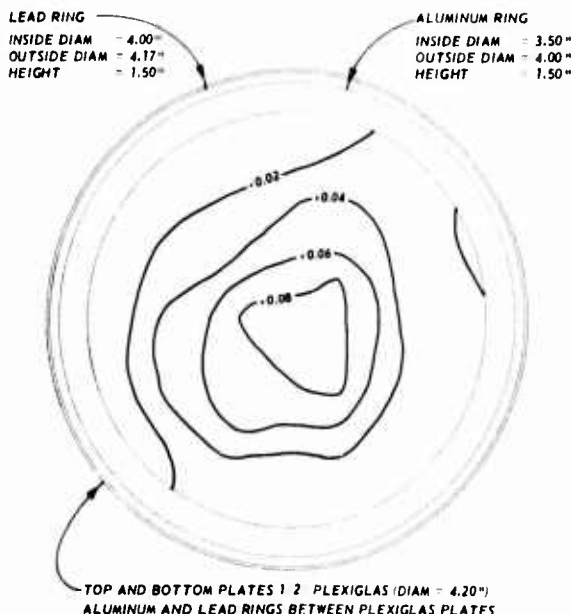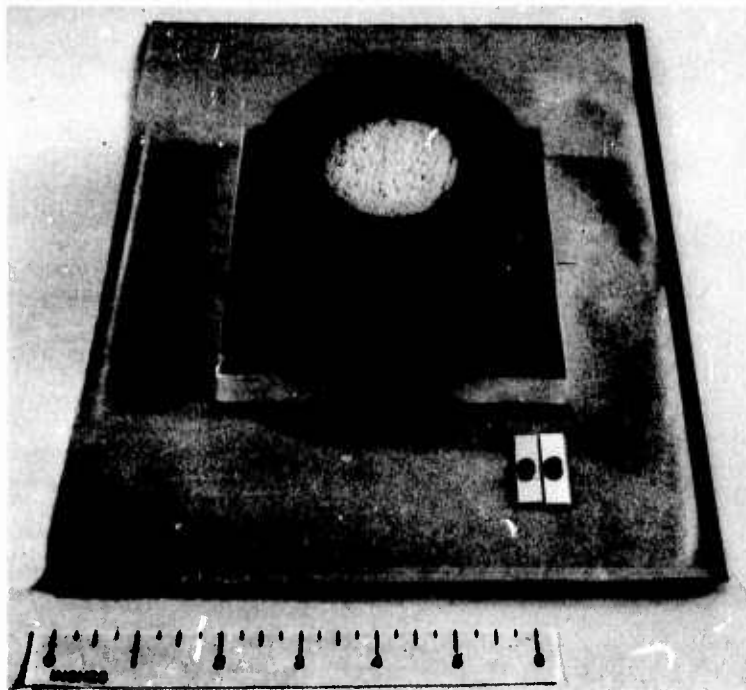and film density variations

S/36-2

a. Model

ALUMINUM RING
INSIDE DIAM = 3.50"
OUTSIDE DIAM = 4.00"
HEIGHT = 1.50"

LEAD RING
INSIDE DIAM = 4.00"
OUTSIDE DIAM = 4.17"
HEIGHT = 1.50"

ALUMINUM RING
INSIDE DIAM = 3.50"
OUTSIDE DIAM = 4.00"
HEIGHT = 1.50"

+0.02
+0.04
+0.06
+0.08
+0.10
+0.12

+0.02
+0.04
+0.06
+0.08

TOP AND BOTTOM PLATES 1 2 PLEXIGLAS (DIAM = 4.20")
ALUMINUM AND LEAD RINGS BETWEEN PLEXIGLAS PLATES

TOP AND BOTTOM PLATES 1 2 PLEXIGLAS (DIAM = 4.20")
ALUMINUM AND LEAD RINGS BETWEEN PLEXIGLAS PLATES
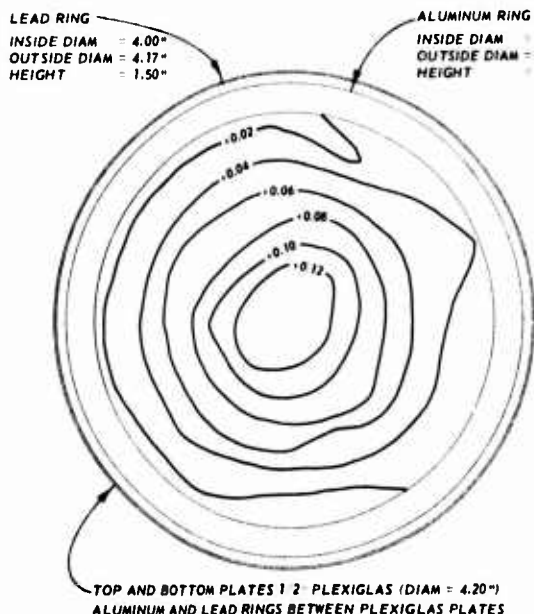
SAND DENSITY 1.77 ; FILM DENSITY 1.04
CONTOURS INDICATE DEVIATION FROM BASE FILM DENSITY
5 MA, 90 KV, 60 SEC, 33-IN. F.D., KODAK TYPE M FILM

SAND DENSITY 1.82 ; FILM DENSITY 1.00
CONTOURS INDICATE DEVIATION FROM BASE FILM DENSITY
5 MA, 90 KV, 60 SEC, 33-IN. F.D., KODAK TYPE M FILM

PATTERN OF RADIATION SCATTER
SAMPLE 95
OTTAWA SAND (20 TO 28 MESH)

PATTERN OF RADIATION SCATTER
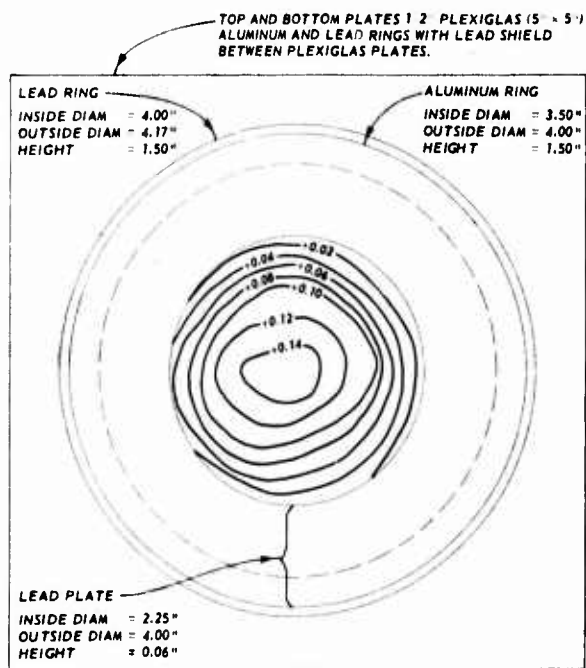SAMPLE 106
OTTAWA SAND (20 TO 28 MESH)

b. Film density variations.
Sand density 1.77

c. Film density variations.
Sand density 1.82

Fig. 7. Model of aluminum ring with lead sheath and circular plexiglas
cover plates, and film density variations

a. Sand model

TOP AND BOTTOM PLATES 1 2 PLEXIGLAS (5 × 5)
ALUMINUM AND LEAD RINGS WITH LEAD SHIELD
BETWEEN PLEXIGLAS PLATES.

LEAD RING
INSIDE DIAM = 4.00"
OUTSIDE DIAM = 4.17"
HEIGHT = 1.50"

ALUMINUM RING
INSIDE DIAM = 3.50"
OUTSIDE DIAM = 4.00"
HEIGHT = 1.50"

LEAD PLATE
INSIDE DIAM = 2.25"
OUTSIDE DIAM = 4.00"
HEIGHT = 0.06"

SAND DENSITY 1.70, FILM DENSITY: 0.98
CONTOURS INDICATE DEVIATION FROM BASE FILM DENSITY:
5 MA, 90 KV, 60 SEC. 33-IN. F.D., KODAK TYPE M FILM

PATTERN OF RADIATION SCATTER
SAMPLE 70
OTTAWA SAND (20 TO 28 MESH)

b. Film density variations

Fig. 8. Sand model with aluminum ring, lead sheath,
and lead partial cover, and film density variations

over a tenth of a film density unit. However, the degree of uniformity was not as great as in the preceding cases where a lead cover plate was not used. The overhang in the lead plate allows radiation scatter from within the radiated sand to be lost laterally by absorption into the peripheral sand mass. Thus, the gradient of the residual film density values is increased slightly. However, some soil models may require lead windows of this sort in order to be examined effectively during the progressions of tests. For such purposes, the technique may be regarded as likely to be satisfactory.

36. It follows that for successful radiation experiments, models must be designed with sidewalls, and sometimes with partial covers, of high radiation absorptive materials in order to reduce radiation gradients in the film images.

Film Processing and Reading

37. Film processing for these experiments was done with a Pako Corporation Packorol-B Film Processor, model 17-1. An automatic film processor, such as this one, controls temperature, time, and chemicals. If handled properly it can do an excellent job of developing film exactly the same, time after time. There are, however, limitations that should be understood. The problems that are involved are common to all film processing.

38. The film consists of a transparent cellulose acetate base material uniformly coated with a silver bromide gelatin emulsion that is sensitive to light. The film is placed in a developer that reacts with the exposed portion of the emulsion and causes a darkening that depends on the amount of exposure. A fixative removes the unexposed areas of sensitive emulsion, and then a rinse removes all the remaining chemicals.

39. The first step, that of developing, is the most crucial and sensitive with respect to the measurement of film density. There are four basic factors affecting development and its effect on film density: time, temperature, chemicals (replenishment), and accessibility of chemicals to the film emulsion (agitation).

19

40. The whole process involves a chemical reaction. The more time, the greater the reaction. The higher the temperature, the greater the reaction. The higher the concentration of chemicals, the greater the reaction. The greater the accessibility of the developer to the film, the greater the reaction. The fixing should be long enough to remove light-sensitive chemicals, and the rinse or wash should be long enough to remove all chemicals. These factors are held constant by the film processor.

41. Three factors, time, temperature, and agitation, were held very constant. The fourth factor, replenishment, was not so well controlled. Most film density variations were due to vagaries in replenishment.

Temperature

42. The temperature of the developer in these experiments was held at 80 F. Checks at various times during the experiments showed that temperatures never measured 81 or 79 F. Thus, the temperature variation was almost negligible   However, a variation of 1 F from 80 F would result in a variation equivalent of about 3 or 4 sec in terms of development time. Total time in the film processor was 105 sec. This would amount to about 3 percent fluctuation in time.

Time

43. Time in the developer was regulated by the control on the feed rate of the film. The radiographs were run at 20 in./min. They traveled 35 in. in 105 sec. This travel or speed was controlled by a free moving dial, with no definite "clicks." The speed was measured or determined by a meter reading in 2-in./min units. The control seemed sufficient to keep the rate of speed within a small fraction of an inch per minute.

Agitation

44. The third factor, agitation, was held extremely constant. The film moved through the developer between rollers at a rate of 20 in./min. Pumps that delivered maximum flow at all times were in operation throughout the film processing. In this way the availability of fresh chemicals to the surface of the film remained patterned and uniform.

Replenishment of chemicals

45. The fourth factor, the replenishment of the chemicals, was

20

also regulated by the machine. As the film entered the machine, a micro-switch was actuated and it in turn activated the replenishment pumps, which pumped new developer solution into the developer bath. After the film passed the microswitch, the switch shut off and the replenishment pumps stopped. The rate of replenishment was regulated at the flowmeter with the replenishment rate controls, which are calibrated in cubic centimeters per minute.

46. The rates were determined by the chemical manufacturer. Slight adjustments were made on these rates on the basis of processed professional process-control strips. Once a consistent replenishment rate was regulated, there was no need for further adjustments.

47. All things being constant, the chemical replenishment is added on the basis of the length of the film put into the machine and removed on the basis of amount and area of exposure. This inequality could be meaningful. Consider two groups of film. One is composed of overexposed 14- by 17-in. film. The other is underexposed 4-1/2- by 17-in. film. Besides having fewer chemicals removed because of exposure, the lesser area would multiply this effect. Meanwhile, as the film is of the same length, the replenishment is the same. Consequently the possibilities exist for inequalities in chemical development.

48. This problem was handled by processing a Kodak B/W professional process-control strip with each sheet of radiographic film. These control strips were then measured using a photodensitometer, and adjustments were made arithmetically to adjust the film values to a control condition. Deviations observed in these experiments did not exceed 0.06 of a film density unit. Most were 0.03 and under. Variations of this order were regarded as linear functions, thus allowing adjustments to be made arithmetically. Variations of 0.10 or greater were regarded as excessive and would not have been corrected in this manner. Such values would have had a nonlinear rate of change that would have resembled the film characteristic curves that relate film density to exposure time.

49. A limitation on accuracy exists in the photodensitometer itself. A MacBeth Quantalog Densitometer model TD100 was used for these experiments. The instrument has three apertures; sizes are 0.0312,
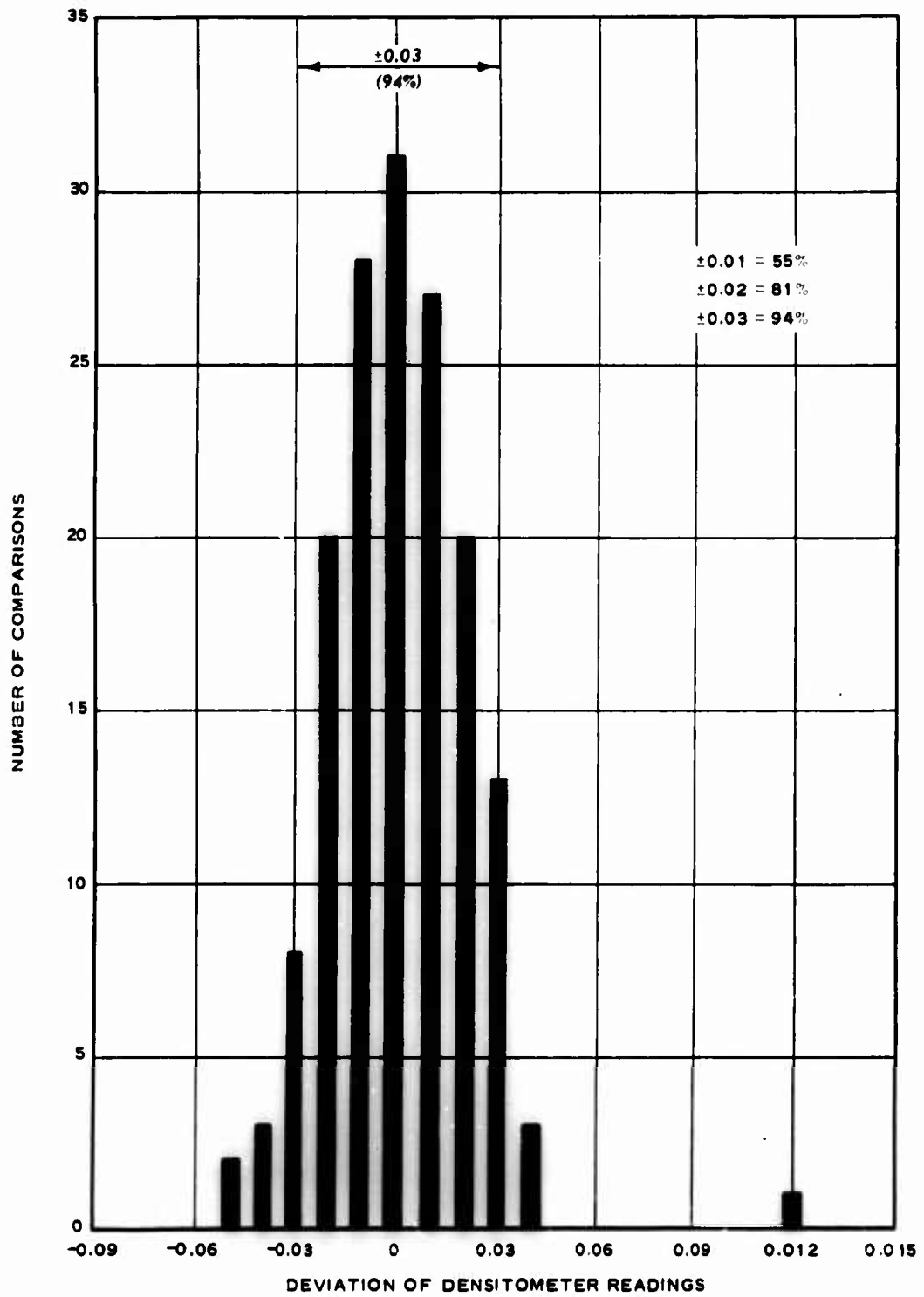
21

Fig. 9. Range of error in a point-reading photodensitometer

0.0787, and 0.118 in. The densitometer is calibrated to utilize the
smallest aperture. The graininess of sand radiographs would present a
problem to the small aperture, which has an area of about 0.0008 sq in.
This tiny area could present differences in the light passing through
light and dark areas of a grain imprint. Consequently, the largest aper-
ture was used to alleviate this problem. The area of the large aperture
is about 0.0437 sq in., an increase in area of about X55.

50. The densitometer was calibrated with the small aperture utiliz-
ing a reading strip with numerous frames of film densities.

51. Fig. 9 shows the range of error in film density units obtained
by measuring and remeasuring a group of 156 standard film strips. Remeas-
uring was done on different days. Contributions to error are deteriora-
tions in the light source in the photodensitometer and vagaries in the
calibration of the instrument. The range of the instrument is $\pm$0.03 of a
film density unit.

Image Control Disks

52. Using film process-control strips is a check on chemical de-
velopment, but it does not check vagaries in the electrical input to the
X-ray tube. A method that checks both energy variation and chemical de-
velopment is to place a standard metal disk in each exposure. The disk
image can then be measured with the photodensitometer, and adjustments in
densitometer readings can be made for the model whenever necessary.

53. In order to interpret soil density in a model from its radio-
graphic image, a calibration curve is necessary. Such a curve relates
film density in the radiograph to its corresponding soil density.

54. To make a calibration curve, one must prepare several speci-
mens of the same soil as that in the model. The specimens must be uni-
formly packed but of different measured densities. They must be in con-
tainers in which edge effects are at a minimum. In this experiment, the
specimens were contained in aluminum rings with lead outer sheaths. The
time and energy levels of exposure must be the same in the calibration as
those intended in the model. The thickness of material radiographed for
the calibration must be the same as that for the model.

55. The calibration curve made for silt (Vicksburg loess) is shown
in fig. 10. The loess was made uniform by passing it through a 200-mesh
sieve and removing all concretionary matter. The resulting material is
90 percent silt and 10 percent clay. Exposure was at 5 ma, 90 kv, at
60 sec with a 33-in. focal distance, on Kodak type M film. Film density
readings around the perimeter of the specimen were averaged to get a
value that had minimum scatter and was comparable from one run to another.
The curve is based on six measured specimens.

56. The calibration curve for sand (Ottawa sand, between 20 and 28
mesh) is shown in fig. 11. Exposure and film density readings were made
under the same conditions as those for the silt. The curve is based on
ten points. In addition, four unknowns were run. These were first plot-
ted on the calibration curve to determine the soil density, then they
were checked by weighing. The determinations were accurate within 3
percent.

57. It should be remembered that any change in the exposure condi-
tions will produce entirely different calibration curves. Fig. 12 shows
an alternate curve for the same sand. Exposure was at 10 ma and 75 kv in-
stead of the previous 5 ma and 90 kv. The curve is essentially a
straight line as before but its slope is different. Care must be taken
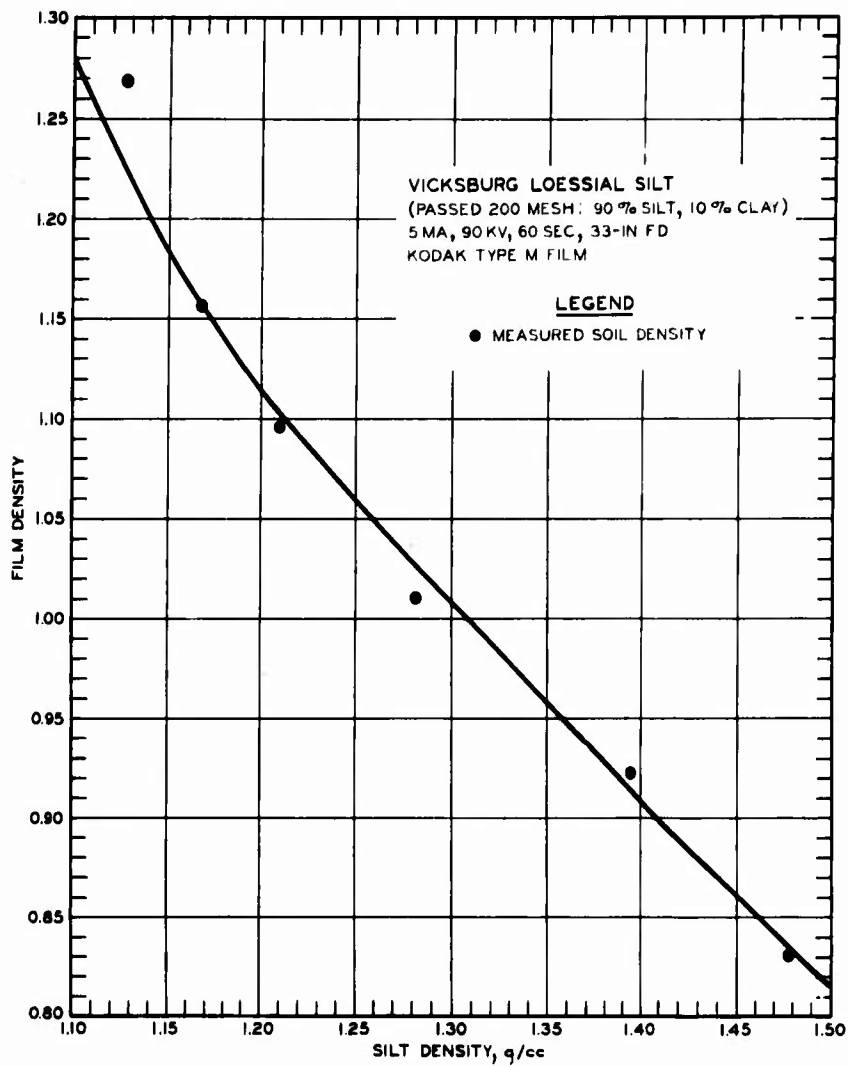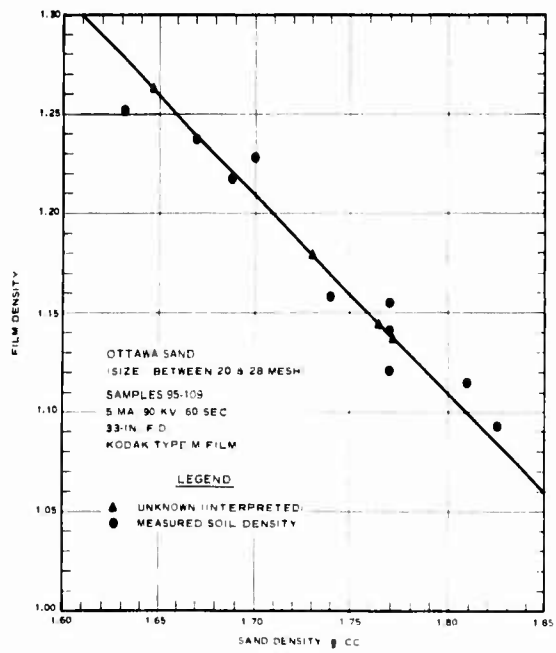to make the exposure of the model as identical as possible with the

24

Fig. 10. Calibration curve: film density to soil
density. Silt: 1.50 in. thick

Fig. 11. Calibration curve: film
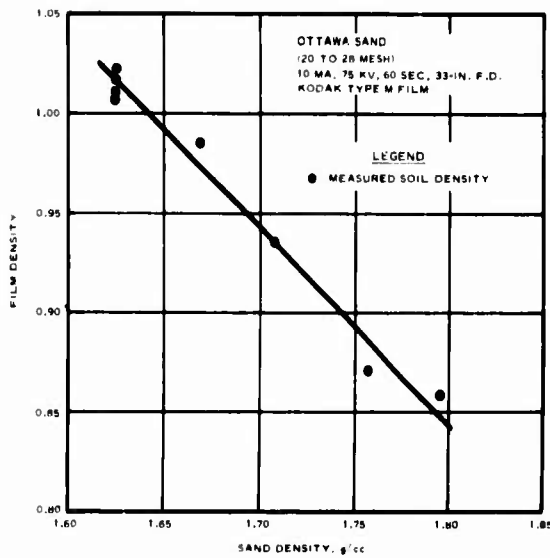density to soil density. Sand:
1.50 in. thick

Fig. 12. Calibration curve: film density to soil density. Sand: 1.50 in. thick. Exposure was varied from that shown in fig. 11

calibration curve for the Vicksburg loessial silt (fig. 10) was based on a 60-sec exposure. Fig. 13 shows the steps followed for converting the 60-sec exposure to 90 sec. This was done point by point along the segment of calibration curve in fig. 10. The new curve is shown in fig. 14. Checks were made experimentally that validated the new curve as being within the same approximate area of accuracy (within 3 percent) as the old one.

59. The advantage of this calculation is that once a calibration is established for a

exposures that were used in making the calibrations.

58. The characteristic curve (film density versus log relative exposure) for the X-ray film can be used to recalculate calibration curves where the exposure has been changed. Fig. 13 shows the characteristic curve for Kodak type M industrial X-ray film. The curve was provided by the Kodak Company and is for a standard 5-min development in a chemical bath. The
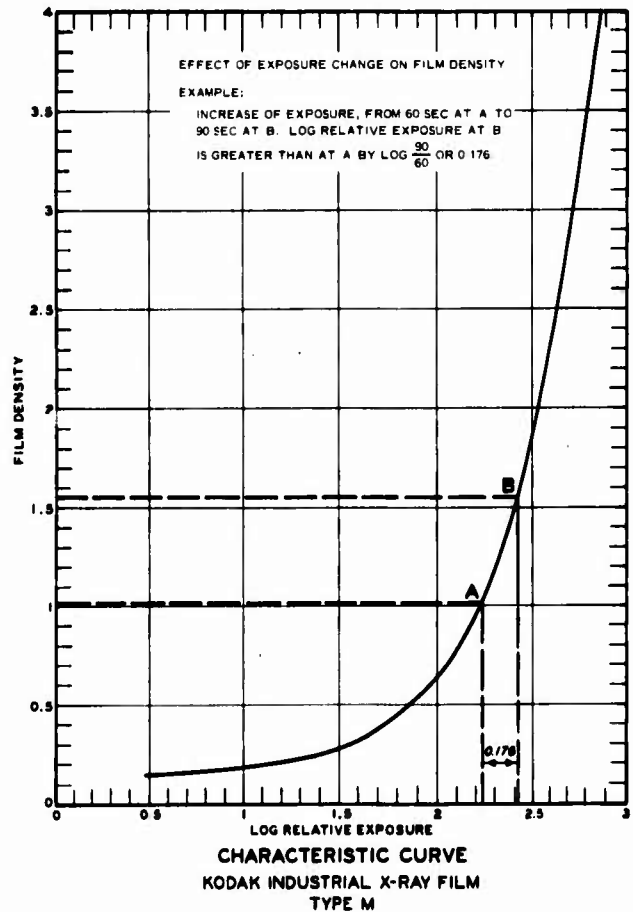
Fig. 13. Calculation of film density change that results from an exposure change

26
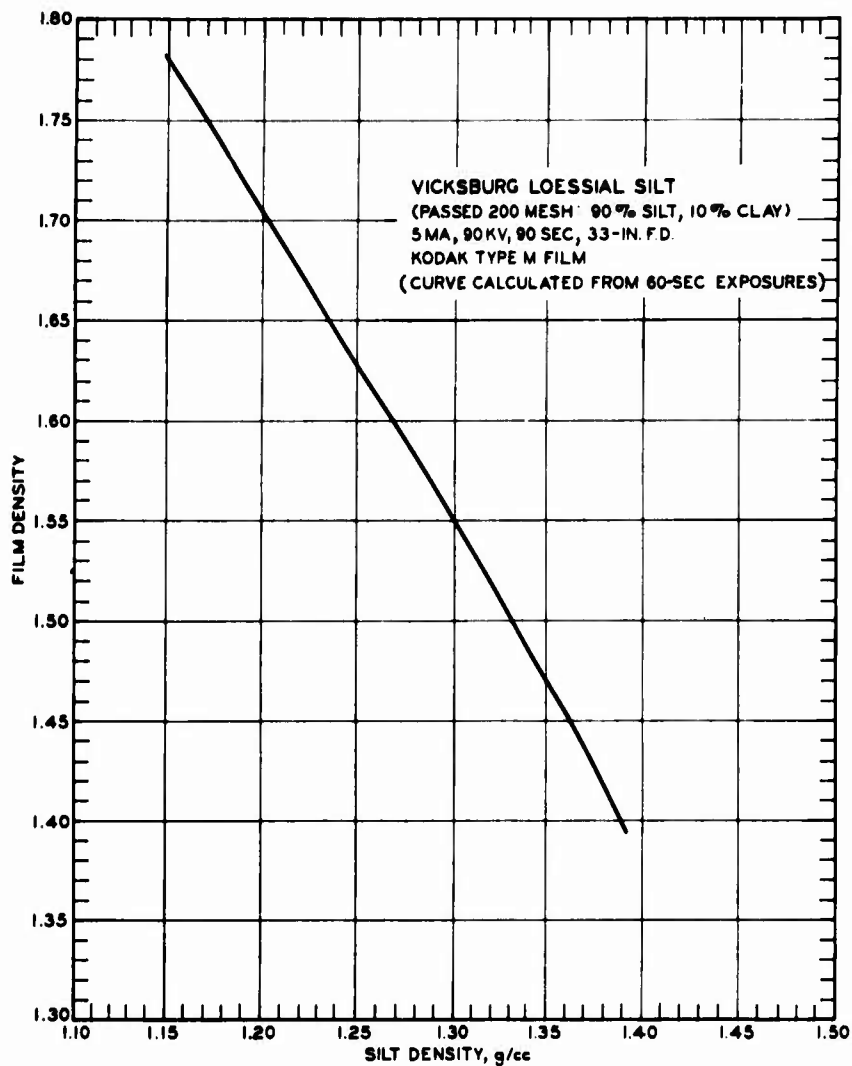
Fig. 14.   Calculated calibration curve for
Vicksburg loessial silt

soil, the exposure times can be varied without the necessity of redoing
the experiments to create a new calibration curve.

60. A series of experiments were run in order to interpret soil density changes induced by loading in a model. The apparatus built for these tests was the squeeze box shown in fig. 15. It was designed to
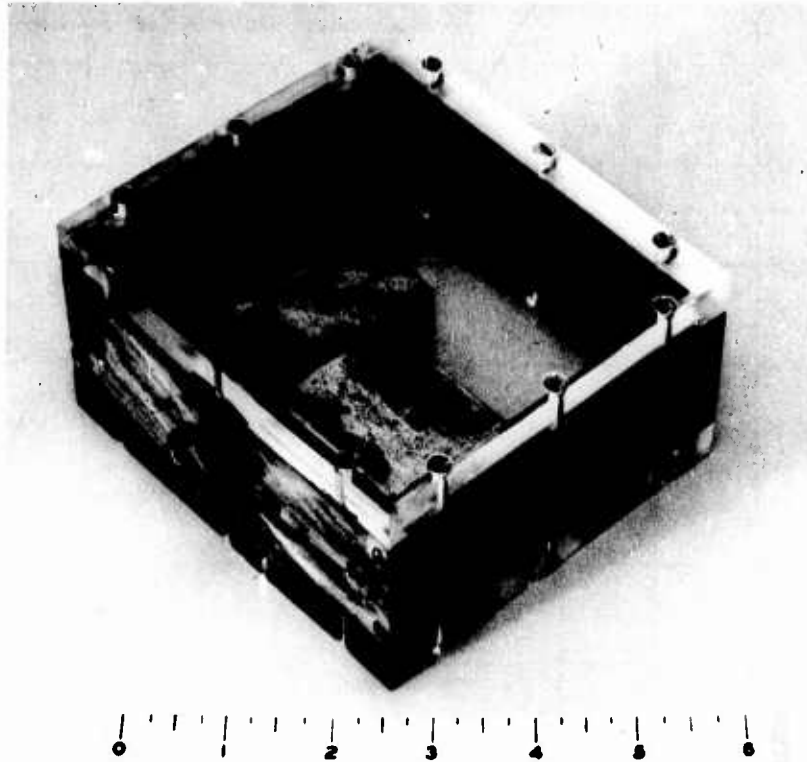
Fig. 15. Soil press designed for inducing soil
density changes by intrusion of a piston. Each
full turn of the screw applied 1/20-in. travel
of the piston

induce soil density changes through intrusion of the piston. Each full turn of the screw applied 1/20-in. travel of the piston. The box was made of steel and was covered above and below with removable plexiglas plates. Inside measurement of the box was 4.50 by 2.50 by 1.50 in. The plexiglas plates were 1/2 in. thick. Tests were run with silt and sand. The film density to soil density relations were those determined in figs. 10 and 12. Radiographic exposures for the press were the same as those for the respective soils for which the calibrations were established.

28

61. Intrusion of the piston was performed in increments of two screw turns, up to a total of eight turns. Beyond eight turns it was found that the induced pressures were high enough to begin deforming the press by bulging the plexiglas plates.

62. The outline of the soil chamber changed with each advancement of the piston making it necessary to run a separate control radiograph for each of the two-, four-, six-, and eight-turn test conditions. In that way the changing scatter pattern that was associated with the changing test chamber was monitored.

63. The controls were run as a set beginning with the eight-turn condition and working down to the zero-turn condition. The piston was positioned first. Then the soil chamber was loaded. Loading of the soil chamber was performed with care to ensure as even and uniform a packing as possible. After each soil addition, the box was tapped gently to help distribute the material. When fully loaded the top plexiglas plate was carefully screwed in place, and the press removed to the X-ray unit. Any rough handling, jarring, or even tilting was avoided so as not to disrupt the packing.

64. By use of guides, the film and press were quickly centered under the X-ray beam, and identical positioning for each condition was ensured. A 5/8-in.-thick aluminum disk was used as an exposure control. It was positioned in a precise location on the X-ray film so that its location in the beam was always the same.

65. After each control specimen was X-rayed the press was opened and the soil weighed. With a measurement of the volume inside the press, the soil density was established. The soil density was used to obtain a residual film density to serve as a reference level of film darkness.

66. The zero-turn control specimen was not immediately opened for weighing of its contents. Instead it served as the initial condition for the compressed series. The piston was forcibly advanced by two turns of the bolt and the chamber X-rayed. Then the four-, six-, and eight-turn conditions were run. When the eight-turn condition was complete, the chamber was opened and the contents weighed. A total of nine conditions-- four controls, four compressed conditions, and one initial condition--were

29

run for both the silt (loess) and sand series.

67. Film handling procedures were kept as regular as possible in order to minimize processing effects on film density. All the film came from the same box. All film sheets for each soil type were developed in sequence on a single day.

68. Furthermore, human errors were minimized by using a mechanical unit to process the radiographs. This unit developed, fixed, washed, and dried the radiographs automatically. Each radiograph was accompanied by a standard filmstrip to note any differences in chemical development should they have occurred.

69. Photographic processing of the radiographs marked the end of one phase of the experimental procedure. The other phase consisted of taking film density data from the radiographs. The radiographs were measured by automatic scanning film density and by grid of point readings made with a MacBeth Quantalog Photodensitometer.

Silt Series

70. The silt series was run with a scanning isodensitracer to take film density data from the radiograph. Uncorrected isodensity tracings for a control specimen at eight turns and a test specimen at eight turns are shown in figs. 16 and 17, respectively. The instrument used was that made by Joyce-Loebl and distributed by Tech Ops Corp., Burlington, Mass. A photodensitometer was used to point check the film density units drawn by the isodensitracer.

71. The isodensitracer measures film density on a two-beam principle. One beam passes through the film while another beam from the same light source passes through a gray wedge. The wedge is servo-driven until the two beams are of equal intensity indicated by a null. The wedge position at the null is then a measure of film density. The printout may be interpreted into a series of contour lines connecting points of equal film density. Contours are printed with two types of marks, either dots or dashes. These marks occur in four different colors. Each color group is separated by a blank or white space that serves as an additional
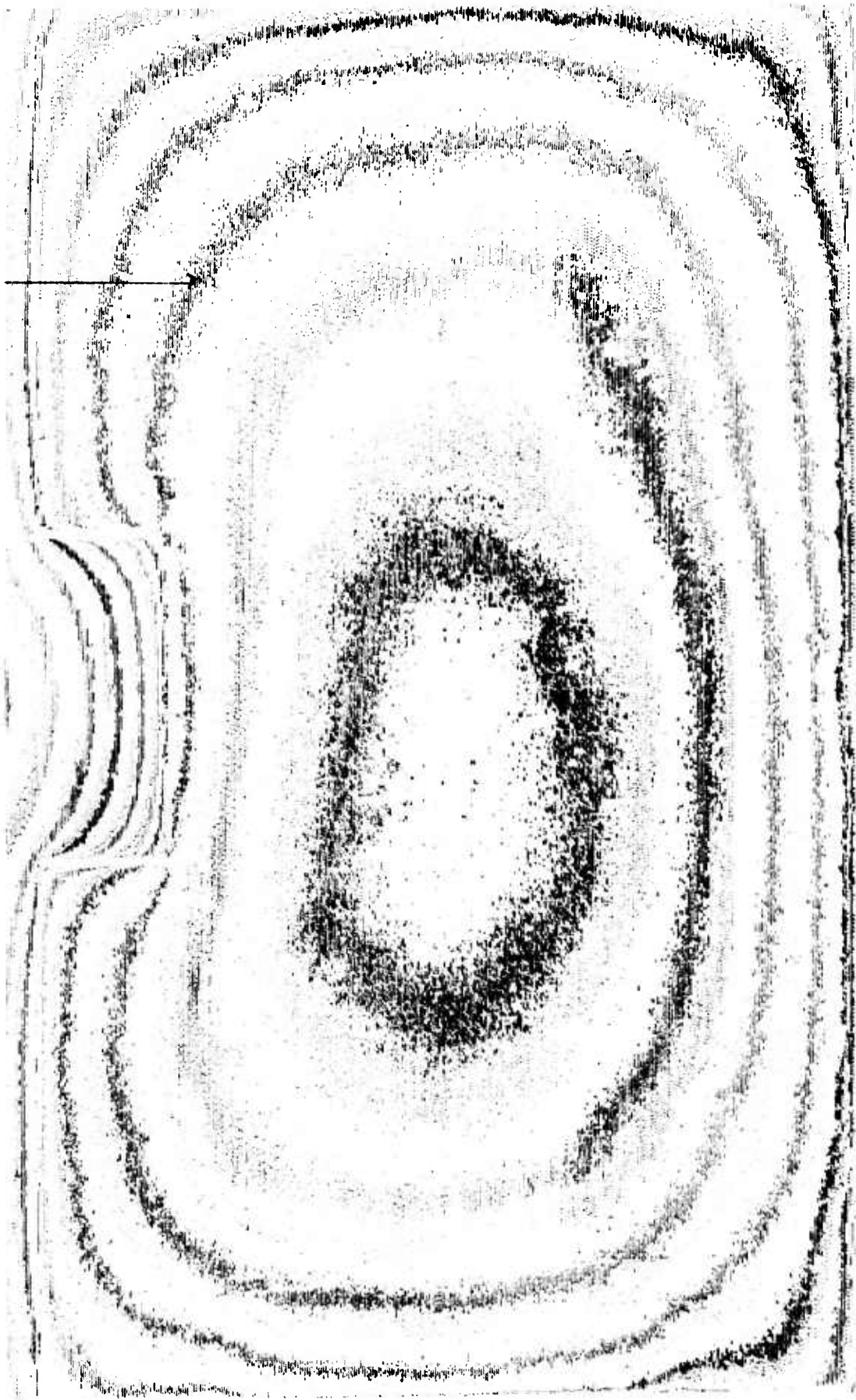
Fig. 16. Uncorrected isodensity tracing for the control specimen, eight turns, Vicksburg loessial silt
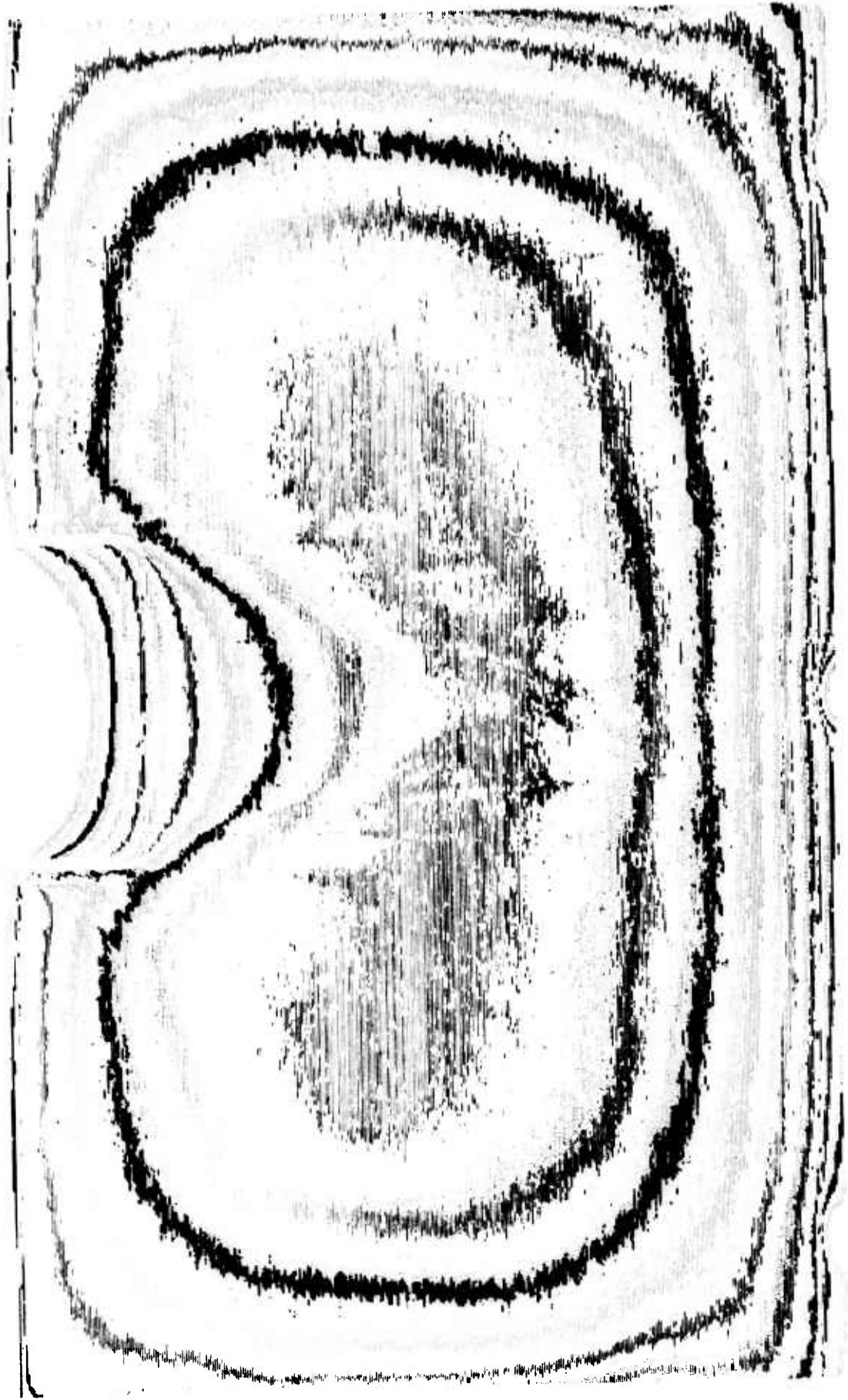
31

Fig. 17. Uncorrected isodensity tracing for the test specimen, eight turns, Vicksburg loessial silt

32

contour zone. The printouts shown in figs. 16 and 17 were made with a magnification of X2.

72. Contours prepared from the isodensitracer were confirmed with the photodensitometer, although the coding was done also with the isodensitracer. Since all other readings in the study were taken with the photodensitometer, including the fundamental film density-soil density calibration plots, it was decided to use the photodensitometer as the one basis for determining absolute values of film density.

73. Figs. 18a-18d show the radiographic film image of the piston compression applied at two turns, four turns, six turns, and eight turns. The prints were made directly from the radiographic film. Thus the darks and lights are reversed. The dark areas in front of the piston represent a densification of the silt. Shear planes show up distinctly in the radiographs at all stages of testing.

74. Film density tracings were made for an initial or pretest condition and for each stage of loading. Further, each stage of loading was radiographed under two conditions: (a) with an advance of the piston and a subsequent packing of the soil so that the soil was not compressed, and (b) with soil that was compressed progressively by advances of the piston. The first set was used as a control for removing scatter at each stage of the piston advance in the actual compressive tests.

75. The measurement and correction steps whereby scatter was removed from the film density readings were as follows:

    a. For each control condition, the soil density was known at the start by calculation from the volume of the test chamber and the weight of soil. This known value was used to check the value determined from the film density and the calibration curve. The two checked with considerable precision, within a 3 percent soil density range of error. The results showed that experiments could have been run without these initial soil density determinations.

    b. Film densities were measured for each test stage and for each corresponding control specimen. A sample measurement is shown in fig. 19. A grid with 148 points was used for each sheet of film.

    c. Measurements of the aluminum control blanks were made on a grid of nine points for each sheet of film. The values for the blanks were averaged. The differences from one sheet
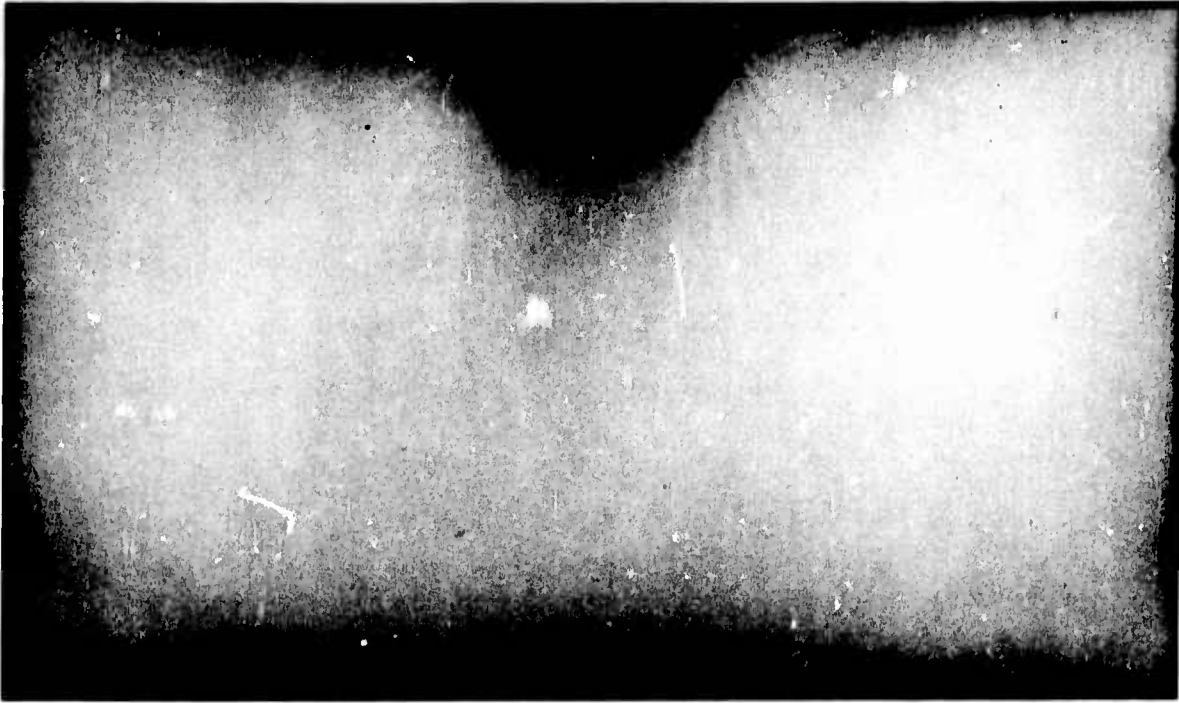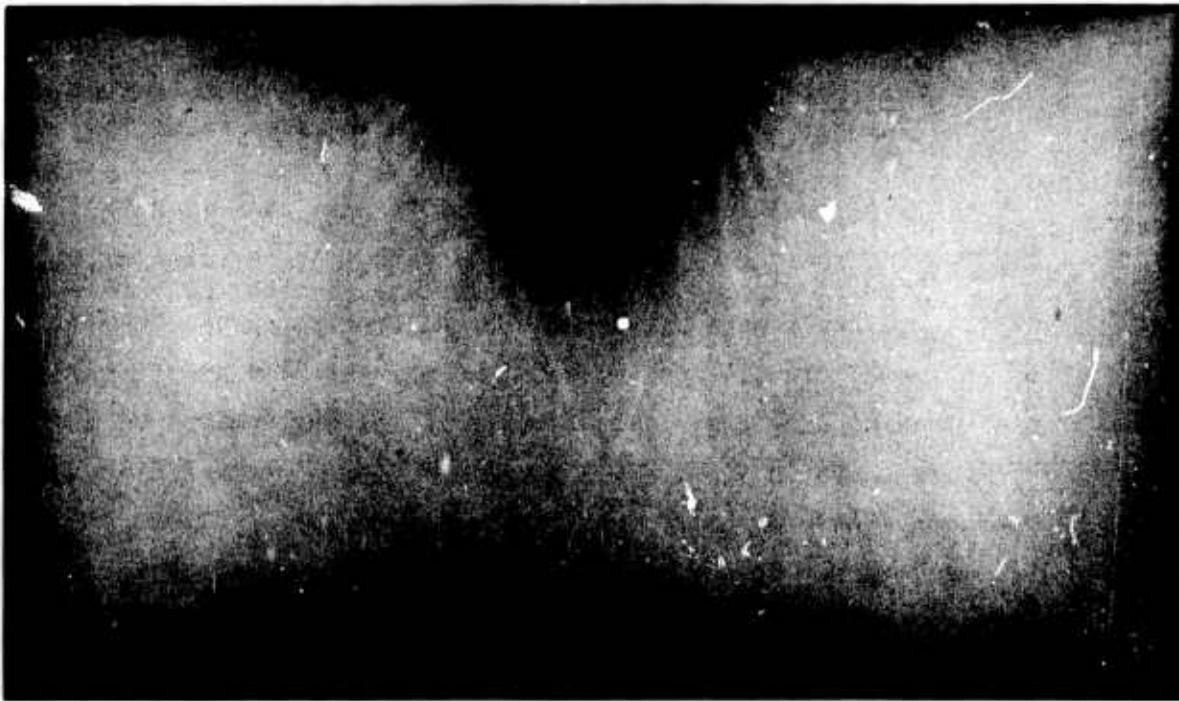
33
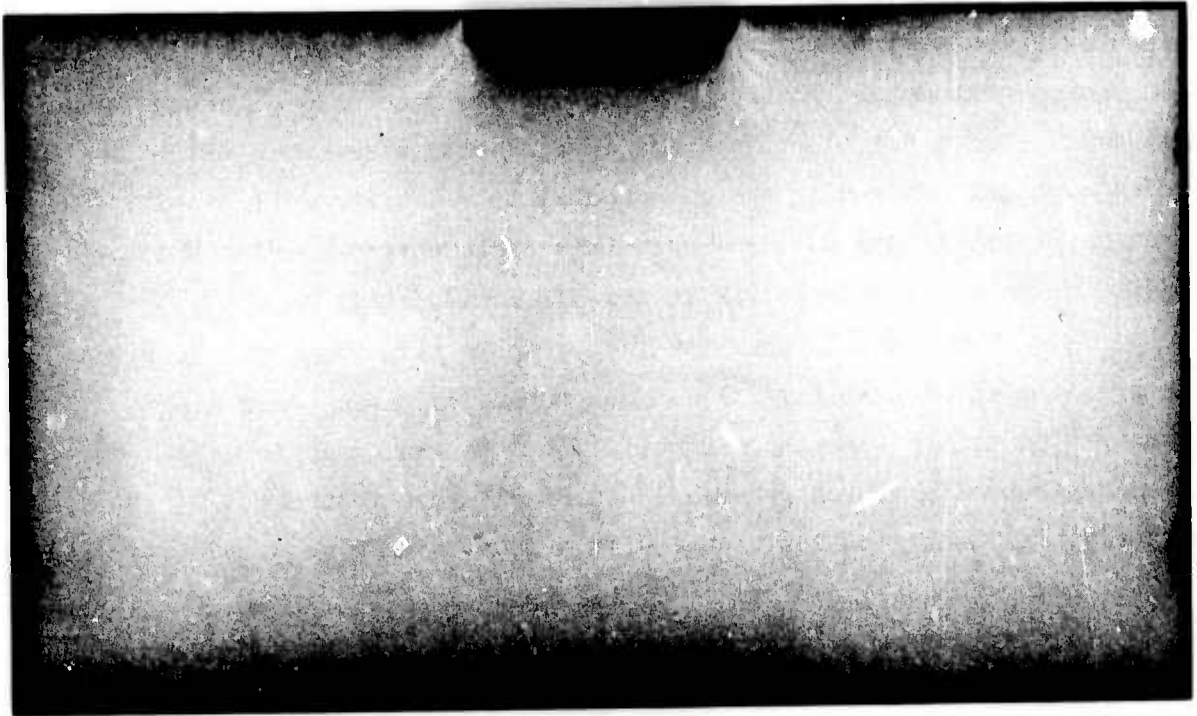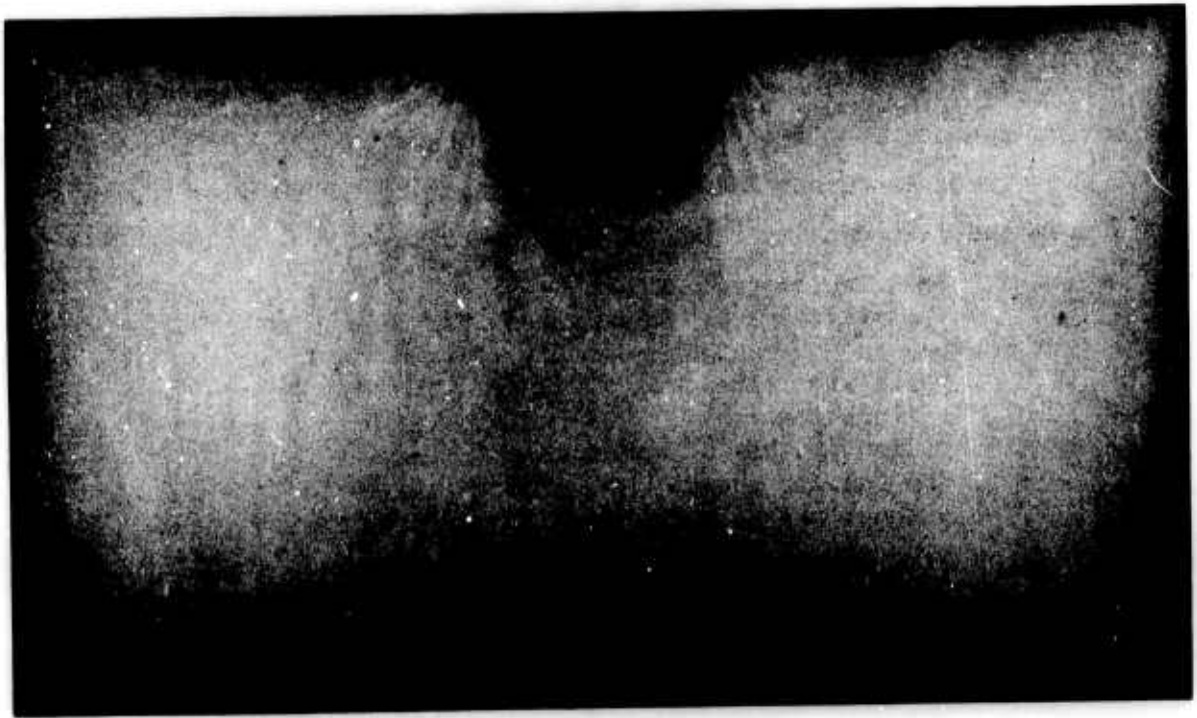
a. After two turns

b. After four turns

Fig. 18. Radiographic prints of silt in soil press after two, four, six, and eight turns of piston (sheet 1 of 2)

c. After six turns

d. After eight turns. (Note densification of the silt before the piston.
    Note also the development of shear planes in the silt.)

Fig. 18 (sheet 2 of 2)

35

1.10	1.12	1.15	1.16	1.16	1.13						1.14	1.15	1.15	1.13	1.11	1.09
1.13	1.18	1.21	1.22	1.26	1.25	1.28	1.20	1.17	1.20	1.27	1.24	1.25	1.22	1.20	1.18	1.12
1.16	1.22	1.24	1.27	1.30	1.32	1.33	1.30	1.28	1.28	1.32	1.29	1.29	1.26	1.23	1.21	1.14
1.18	1.23	1.28	1.30	1.33	1.34	1.37	1.35	1.35	1.36	1.39	1.33	1.32	1.29	1.26	1.25	1.18
1.20	1.25	1.29	1.31	1.34	1.36	1.38	1.38	1.39	1.39	1.37	1.35	1.33	1.31	1.27	1.25	1.17
1.20	1.24	1.31	1.31	1.34	1.36	1.36	1.38	1.38	1.39	1.36	1.34	1.34	1.31	1.28	1.24	1.18
1.18	1.24	1.28	1.30	1.32	1.34	1.35	1.36	1.36	1.36	1.35	1.32	1.31	1.30	1.26	1.22	1.17
1.17	1.22	1.24	1.26	1.28	1.31	1.31	1.32	1.33	1.33	1.32	1.30	1.29	1.26	1.25	1.21	1.16
1.14	1.17	1.20	1.21	1.24	1.26	1.25	1.26	1.26	1.26	1.25	1.25	1.24	1.22	1.19	1.16	1.13

Fig. 19. Film density measurements for an eight-turn test specimen, sand. Measurements are in uncorrected film density units

of film to another were brought to a common average for the blanks.

d. The film density values for the test specimens were compared with those from the control specimens. Residual values of their differences were calculated by subtraction. The residual values were added to the base value for the soil.

e. The resulting film density values were contoured.

f. The contoured values for film density were interpreted for their corresponding values for soil density by reference to the previously developed calibration curve.

76. A series of soil density contours for the silt specimen from its initial condition progressively through to the maximum compression at eight turns are shown in figs. 20a-20e. Shear planes have been superimposed by tracings made directly from the radiographs.

77. The pretest condition, shown in fig. 20a, was a special exercise that was made to locate slight inhomogeneities in the original packing of the soil into the model. It was observed that the isodensity tracing was slightly asymmetrical though not because of the X-ray beam pattern. Other specimens of pretest materials showed more nearly perfect
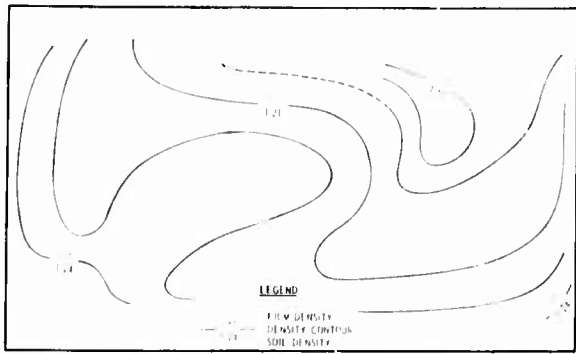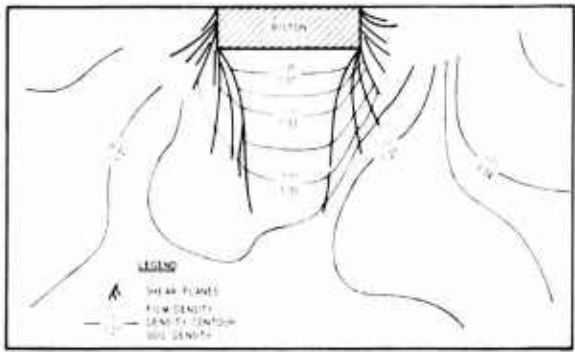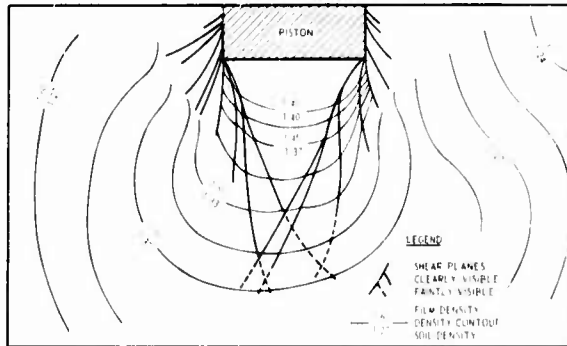
36
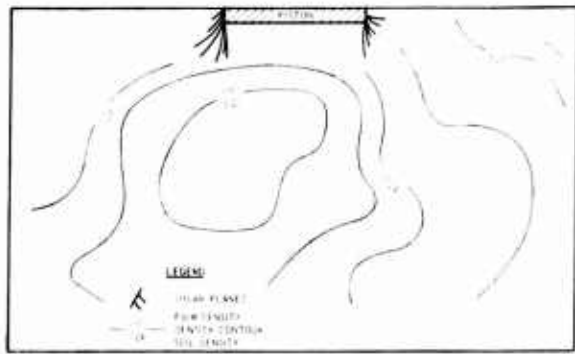
a. After zero turns   b. After two turns
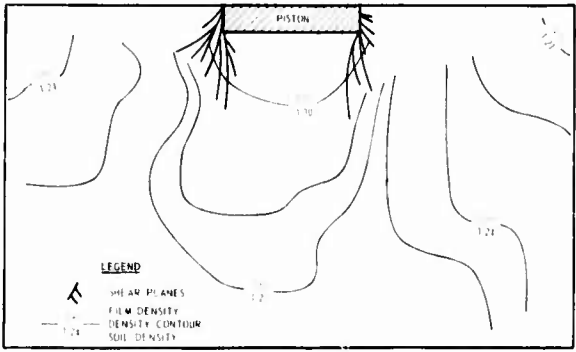
c. After four turns   d. After six turns

e. After eight turns

Fig. 20. Interpreted soil density variations in Vicksburg loessial
silt after zero, two, four, six, and eight turns of piston

37

symmetry. Thus, the asymmetry of the curves was corrected by creating an idealized set of curves based on greater symmetry. Differences were measured. The resulting contours show a slight variation in the density contours on the order of 0.07 of a soil density unit.

78. Figs. 20b-20e show progressively the density changes that were induced. In the final stage of testing, the range of densities within the model is 0.16 of a soil density unit. The greatest change in density from the pretest condition to the final stage is on the order of 0.2 of a soil density unit. The slight asymmetry that was present in the untested condition (fig. 20a) is traceable through the tests to the six-turn condition in fig. 20d. In the final condition (fig. 20e) it has been essentially removed by the adjustments induced by the piston.

79. The inferred shear planes (they may also be localized volume expansions in narrow zones that precede shear) that are shown on the density contour diagrams were traced directly from the appropriate radiographs. The isodensitracer (see fig. 17) does not bring out shear planes in a satisfactory manner.

Sand Series

80. The sand series was prepared and tested in the same manner as that for the silt series. The resulting soil density determinations are shown in figs. 21a-21e.

81. Initially the test specimen had a density variation of 0.03 of a soil density unit. In the final condition, the range was 0.03. The greatest change from pretest to final conditions amounted to 0.09. No shear planes were determinable, and the induced density changes were not concentrated nearest the face of the piston, as were those for the silts, but were distributed much more equitably throughout the specimen.
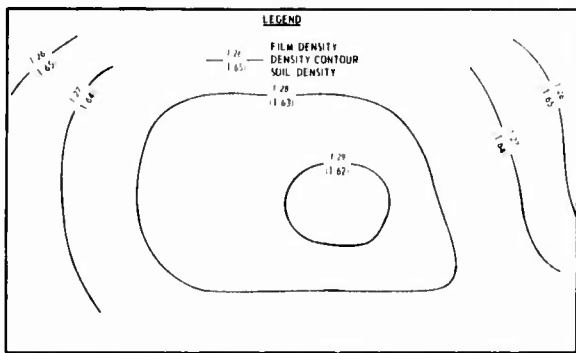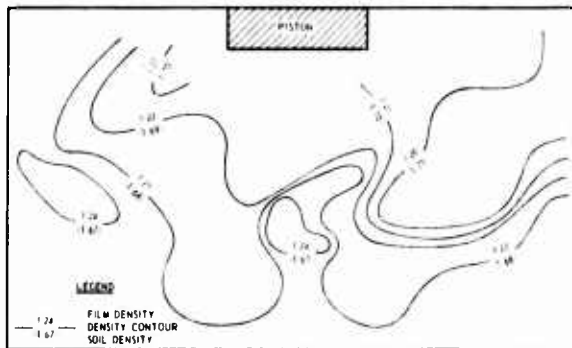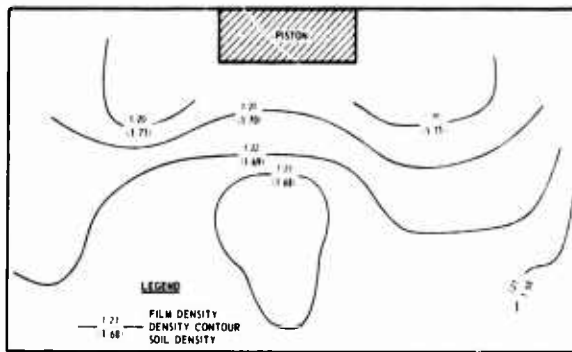
38
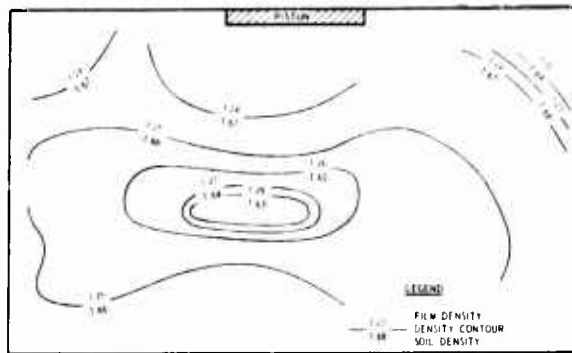
a. After zero turns

b. After two turns
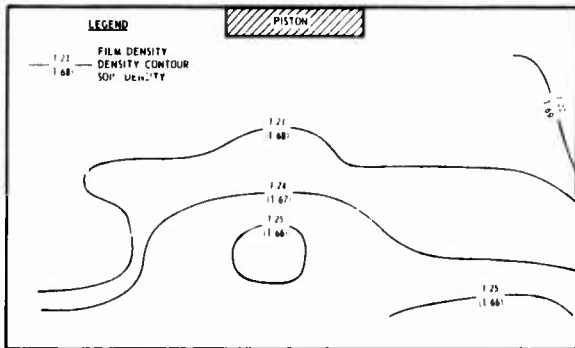
c. After four turns

d. After six turns

e. After eight turns

Fig. 21. Interpreted soil density variations in Ottawa sand after zero, two, four, six, and eight turns of piston

## PART VI: EVALUATION OF DEFORMATION AND SHEAR PLANES

82. Shear zones did not appear in the radiographs for sand. There-
fore, an experiment was run in which lead shot pellets were aligned in a
sand model before the face of the piston, fig. 22a. Piston displacements
at four and eight turns are shown in figs. 22b and 22c, respectively.
Pellets before the piston face were displaced by the piston but were
largely not displaced in relation to each other. However, pellets near
the piston edges were very distinctly pulled apart. These movements are
not seen in the radiographs.

83. Though shear planes were registered in the radiographs for silt,
it is not certain that they showed fully the displacements that occurred.

84. There are ways of enhancing the appearance of shear planes in
radiographs. For example, fig. 23 is a "differential tracing" (Tech Ops
Corp., Burlington, Mass.) of the shear planes in a silt specimen. The
radiograph was scanned with an optical device that registers progressive
differences in film density with a gray tone. However, inflections in
the rate of change of film density are registered more strongly. In this
way the shear planes are highlighted. (Similar devices are made by other
companies, and the method is sometimes called "edge enhancement.") It is
by no means certain that the image in fig. 23 shows all of the shear
planes or fully presents the most important displacements.

85. A silt specimen was also instrumented with lines of lead pel-
lets (fig. 24a) and compressed to four and eight turns. At four turns,
the displacements seem to be without pronounced tearing apart of the
material (fig. 24b). At eight turns, pronounced shear displacements have
occurred (fig. 24c). However, the shear planes are not evident because
of the exposure conditions or possibly for other causes that are not un-
derstood. A further attempt to record the displacements within the silt
was made with a grid of lead pellets (figs. 25a and 25b). The resulting
pellet displacements were plotted on a grid (figs. 26a and 26b). Through
a reconstruction of the shortenings and extensions of the grid it was
possible to document the translations of material within the specimen.

86. Studies of density changes in models would benefit from instru-
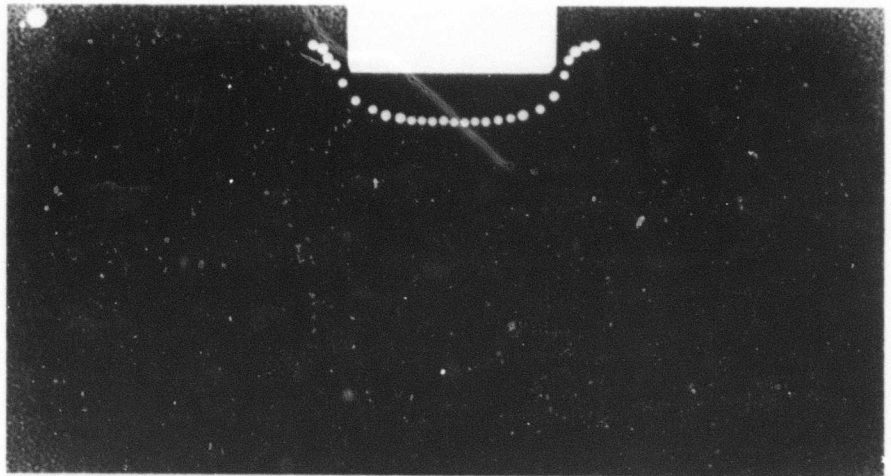menting the models with lead pellets.
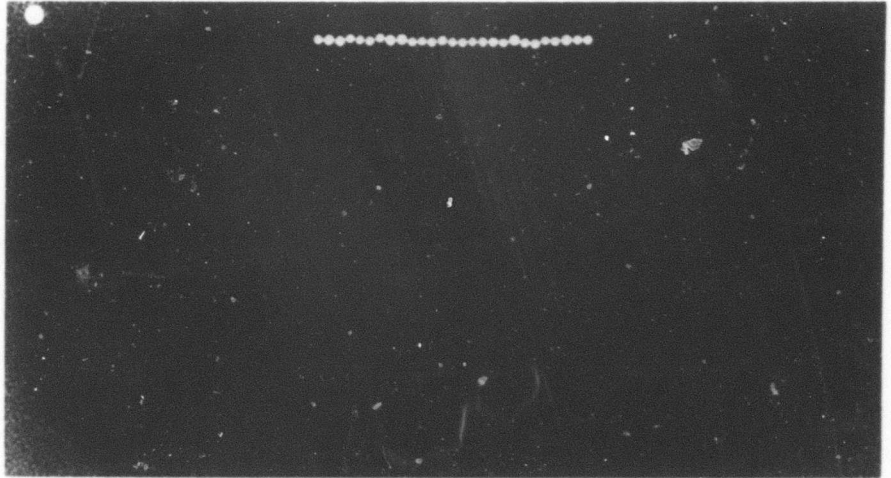
a. At zero turns

Fig. 22. Displacement of lead pellets in model of Ottawa sand after zero, four, and eight turns of piston
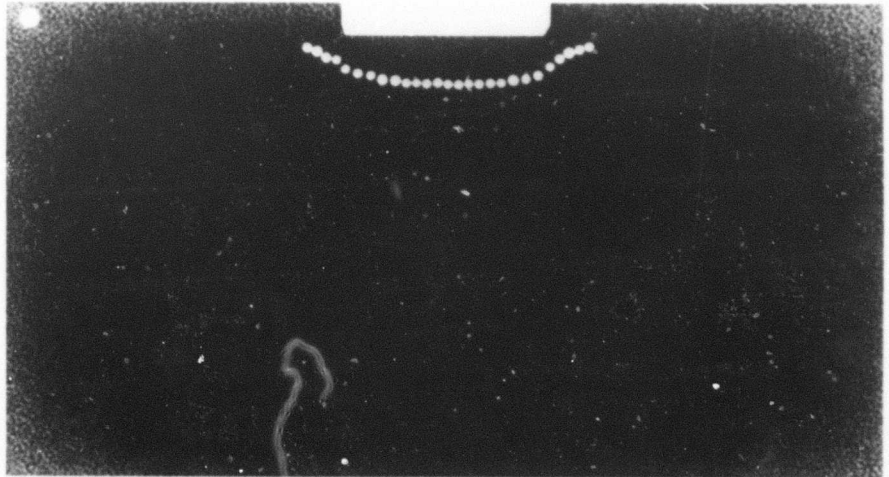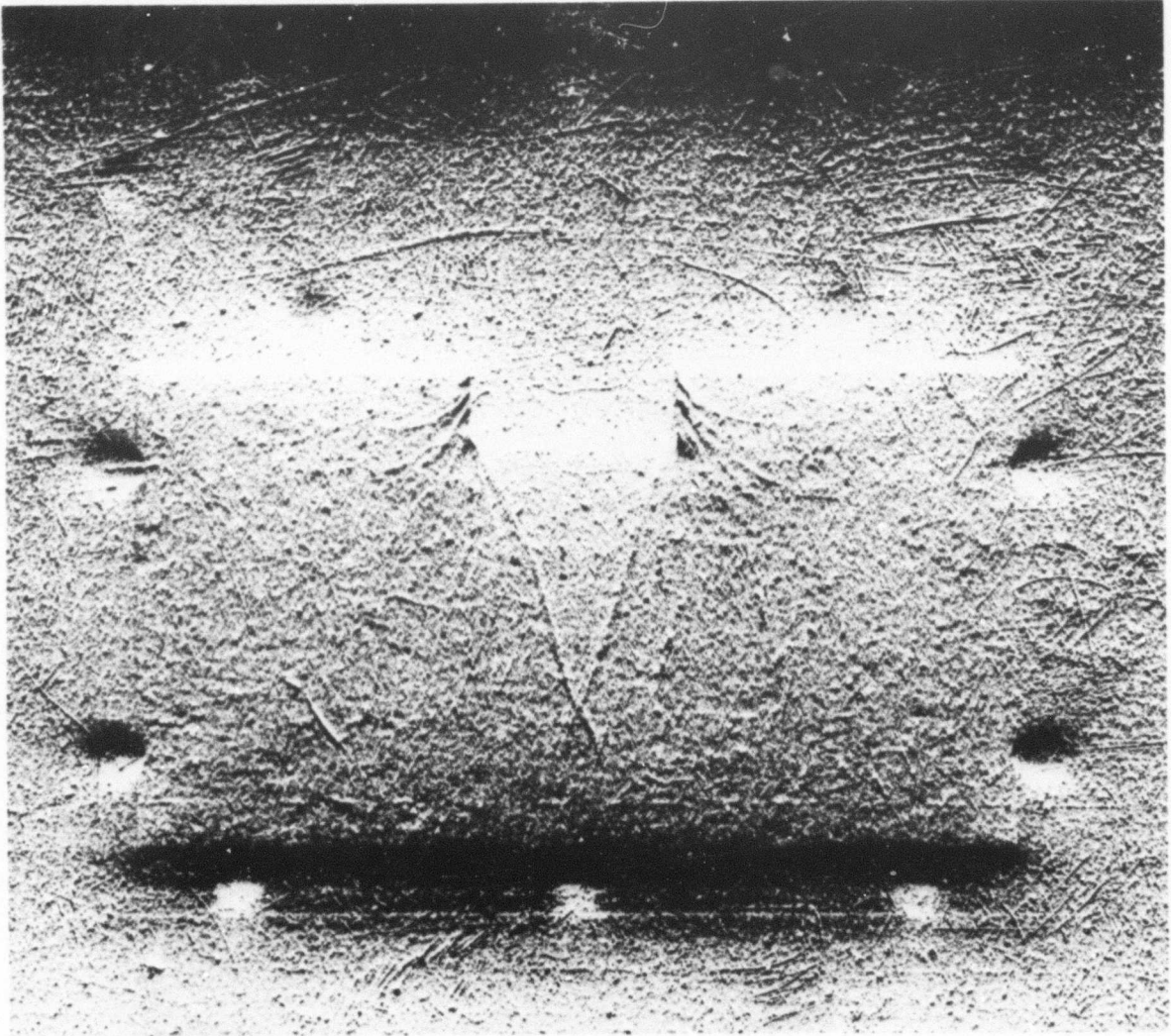
b. After four turns
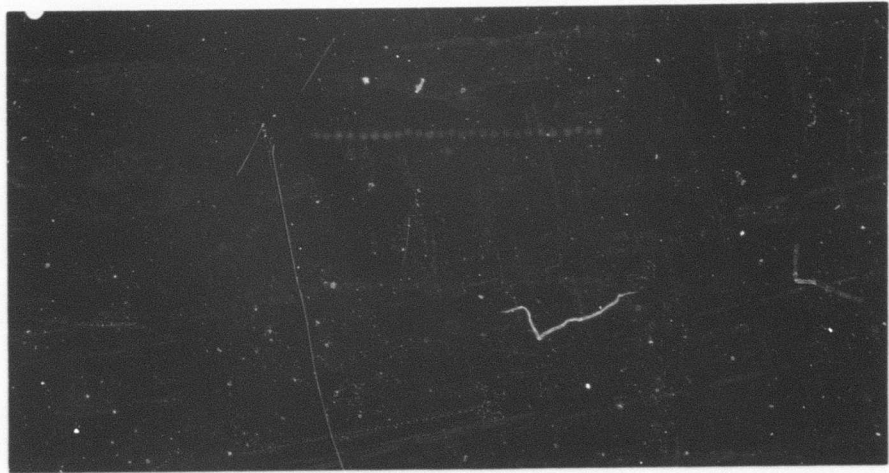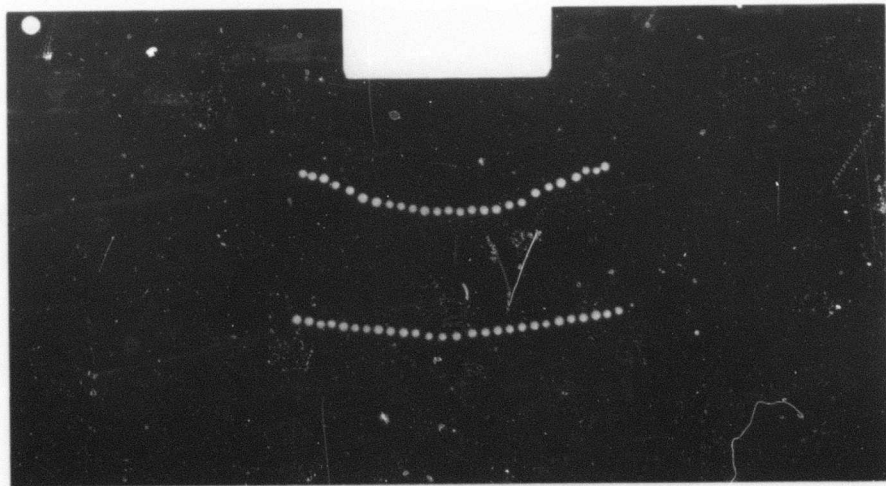
c. After eight turns

Fig. 23. Differential tracing of shear planes in Vicksburg
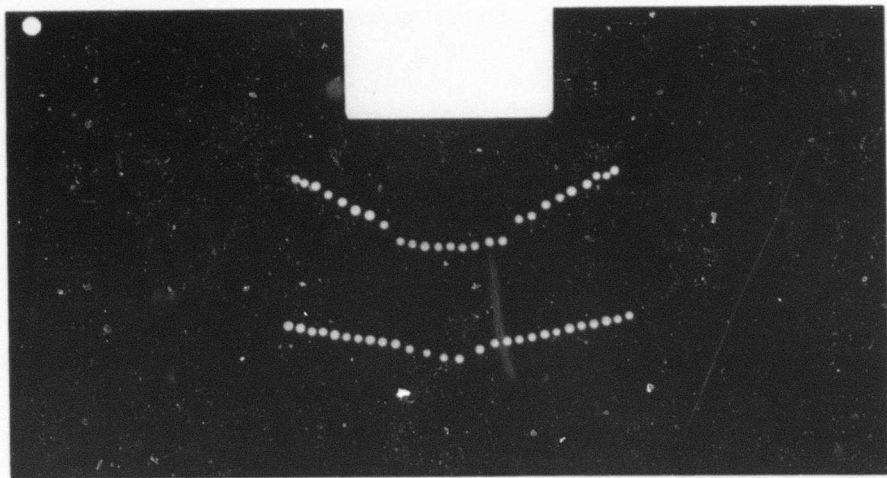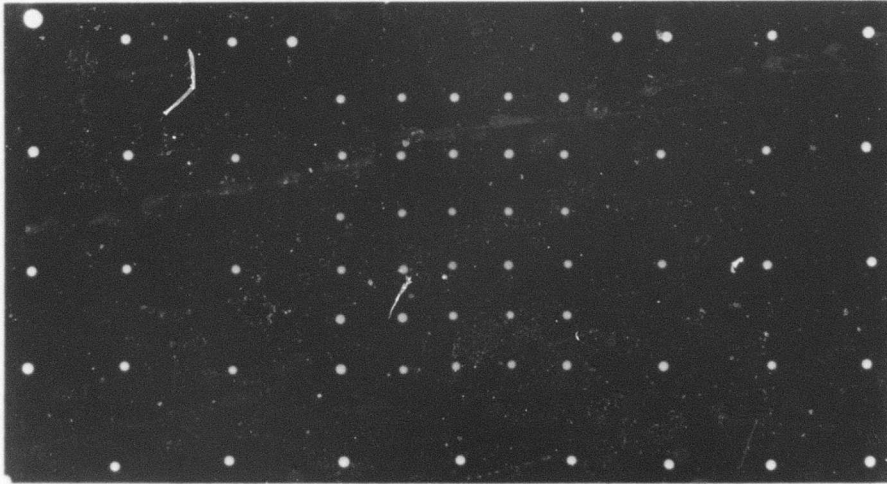loessial silt at eight turns

a.   At zero turns

Fig. 24. Displacement of lead pellets in model of Vicksburg loessial silt after zero, four, and eight turns of piston
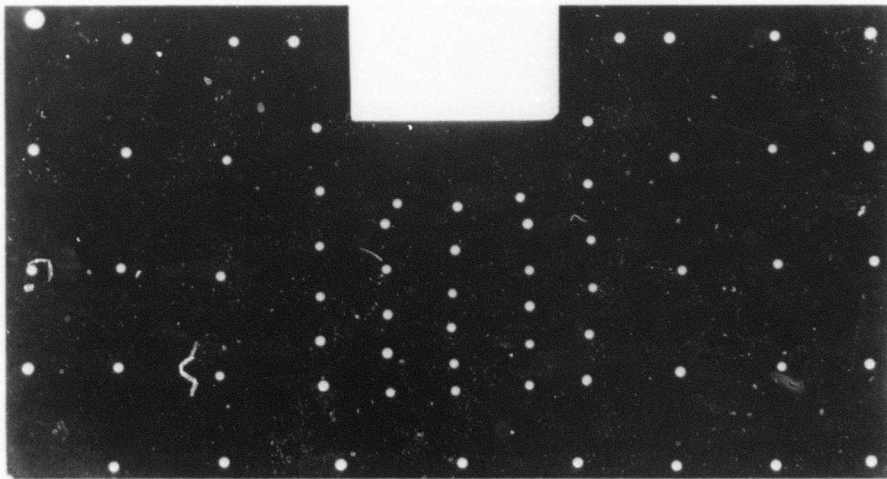
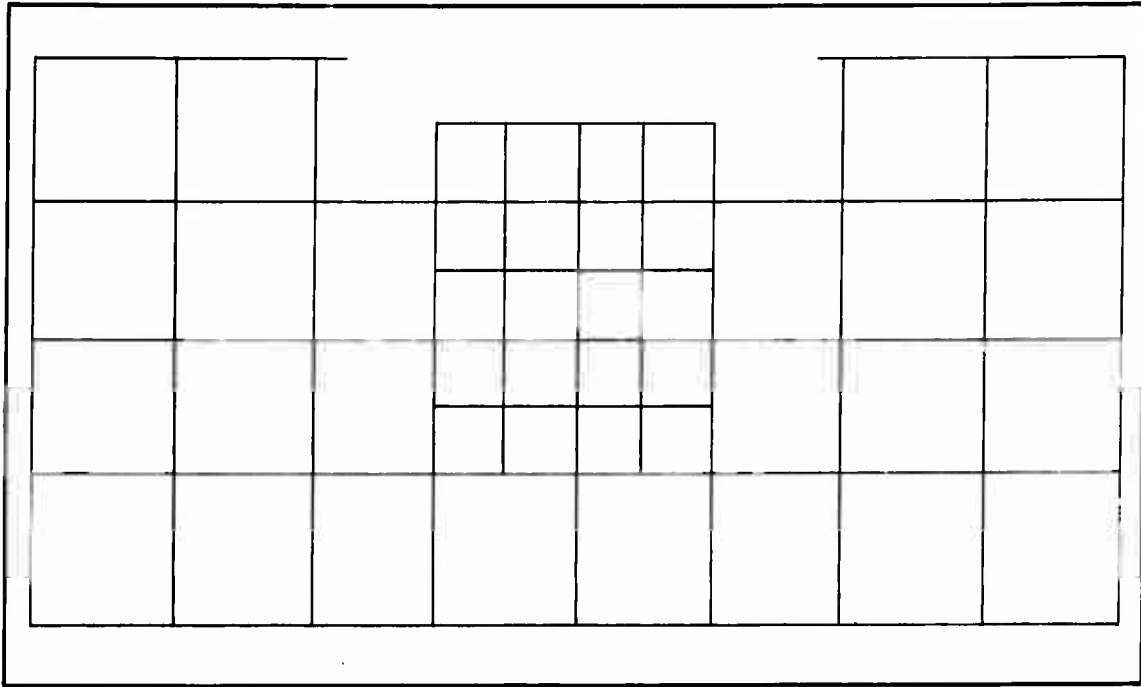b.   After four turns

c.   After eight turns
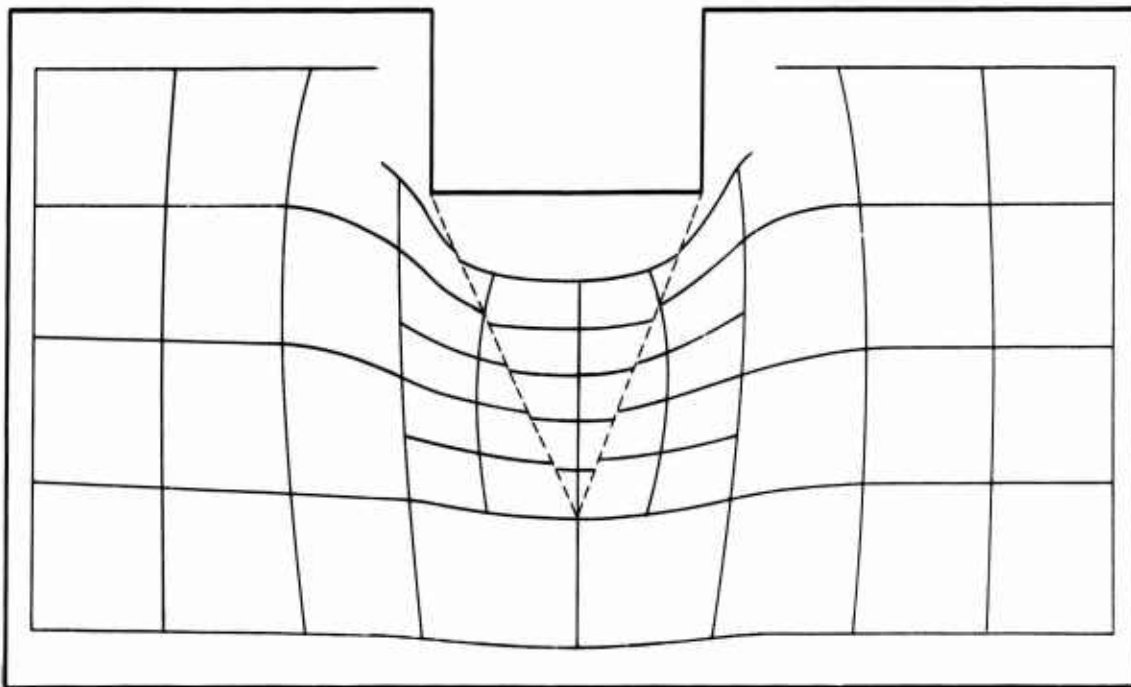
a. Lead pellets in place

b. Lead pellets after eight turns

Fig. 25. Placement of a grid of lead pellets in a model of Vicksburg loessial silt, and displacement of grid after eight turns of piston

a. Grid shown in fig. 25a

b. Grid shown in fig. 25b

Fig. 26. Diagrams of grids shown in figs. 25a and 25b

PART VII: CONCLUSIONS

87. The described tests show that, under proper conditions, X-radiographs can be used to interpret densities in soil models. The method is nondestructive and can be run at various stages of model testing. The most effective means for such testing is with calibration curves that relate radiographic film densities to soil densities. Calibration curves are obtained empirically by test measurements. Once obtained, the curves can be recalculated for changes in the exposure time to radiation. The overall accuracy is approximately 3 percent. Variations within the radiographic image can be measured for tiny areas, even to dimensions in microns, and comparative measures of both film densities and soil densities within an image can be made to hundredths of density units. In this respect, and in its nondestructiveness, the accomplishment of these soil density determinations is far beyond what has been done heretofore.

88. It was found that the shapes of models and the materials of which they are made have important effects on the practicality and accuracy of these determinations.

89. For deformations in models and for analyses of shear, supplementary techniques and instrumentation with lead pellets are needed.